Cosmic Ray Anisotropy with the Telescope Array Experiment

Jihyun Kim (University of Utah)

on behalf of the Telescope Array Collaboration

Cosmic Ray Anisotropy Workshop 2023

2023-05-17

jihyun@cosmic.utah.edu

Outline

- Telescope Array (TA) Experiment
- TA Hotspot
  - Results using 14 years of data
  - Independent dataset analysis
  - Chance probability estimation
- Perseus-Pisces SuperCluster (PPSC) Excess
  - Results using 14 years of data
  - Independent dataset analysis
  - Chance probability estimation
- Summary

Telescope Array Collaboration

USA

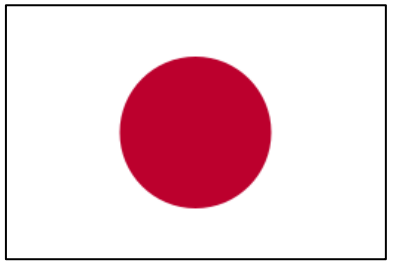

Japan

Korea

R.U. Abbasi,[1] M. Abe,[2] T. Abu-Zayyad,[1] M. Allen,[1] R. Azuma,[3] E. Barcikowski,[1] J.W. Belz,[1] D.R. Bergman,[1] S.A. Blake,[1] R. Cady,[1] B.G. Cheon,[4] J. Chiba,[5] M. Chikawa,[6] A. di Matteo,[7,*] T. Fujii,[8] K. Fujisue,[9] K. Fujita,[10] R. Fujiwara,[10] M. Fukushima,[9,11] G. Furlich,[1] W. Hanlon,[1] M. Hayashi,[12] Y. Hayashi,[10] N. Hayashida,[13] K. Hibino,[13] R. Higuchi,[9] K. Honda,[14] D. Ikeda,[15] T. Inadomi,[16] N. Inoue,[2] T. Ishii,[14] R. Ishimori,[3] H. Ito,[17] D. Ivanov,[1] H. Iwakura,[16] H.M. Jeong,[18] S. Jeong,[18] C.C.H. Jui,[1] K. Kadota,[19] F. Kakimoto,[3] O. Kalashev,[20] K. Kasahara,[21] S. Kasami,[22] H. Kawai,[23] S. Kawakami,[10] S. Kawana,[2] K. Kawata,[9] E. Kido,[9] H.B. Kim,[4] J.H. Kim,[10] J.H. Kim,[1] M.H. Kim,[18] S.W. Kim,[18] S. Kishigami,[10] V. Kuzmin,[20,†] M. Kuznetsov,[20,7] Y.J. Kwon,[24] K.H. Lee,[18] B. Lubsandorzhiev,[20] J.P. Lundquist,[1] K. Machida,[14] K. Martens,[11] H. Matsumiya,[10] T. Matsuyama,[10] J.N. Matthews,[1] R. Mayta,[10] M. Minamino,[10] K. Mukai,[14] I. Myers,[1] S. Nagataki,[17] K. Nakai,[10] R. Nakamura,[16] T. Nakamura,[25] Y. Nakamura,[16] Y. Nakamura,[16] T. Nonaka,[9] H. Oda,[10] S. Ogio,[10,26] M. Ohnishi,[9] H. Ohoka,[9] Y. Oku,[22] T. Okuda,[27] Y. Omura,[10] M. Ono,[17] R. Onogi,[10] A. Oshima,[10] S. Ozawa,[28] I.H. Park,[18] M.S. Pshirkov,[20,29] J. Remington,[1] D.C. Rodriguez,[1] G. Rubtsov,[20] D. Ryu,[30] H. Sagawa,[9] R. Sahara,[10] K. Saito,[9] Y. Saito,[16] N. Sakaki,[9] T. Sako,[9] N. Sakurai,[10] K. Sano,[16] L.M. Scott,[31] T. Seki,[16] K. Sekino,[9] P.D. Shah,[1] F. Shibata,[14] T. Shibata,[9] H. Shimodaira,[9] B.K. Shin,[10] H.S. Shin,[9] J.D. Smith,[1] P. Sokolsky,[1] N. Sone,[16] B.T. Stokes,[1] S.R. Stratton,[1,31] T.A. Stroman,[1] T. Suzawa,[2] Y. Takagi,[10] Y. Takahashi,[10] M. Takamura,[5] M. Takeda,[9] R. Takeishi,[18] A. Taketa,[15] M. Takita,[9] Y. Tameda,[22] H. Tanaka,[10] K. Tanaka,[32] M. Tanaka,[33] Y. Tanoue,[10] S.B. Thomas,[1] G.B. Thomson,[1] P. Tinyakov,[20,7] I. Tkachev,[20] H. Tokuno,[3] T. Tomida,[16] S. Troitsky,[20] Y. Tsunesada,[10,26] Y. Uchihori,[34] S. Udo,[13] T. Uehama,[16] F. Urban,[35] T. Wong,[1] K. Yada,[9] M. Yamamoto,[16] H. Yamaoka,[33] K. Yamazaki,[13] J. Yang,[36] K. Yashiro,[5] M. Yosei,[22] H. Yoshii,[37] Y. Zhezher,[9,20] and Z. Zundel.[1]

[1] *High Energy Astrophysics Institute and Department of Physics and Astronomy, University of Utah, Salt Lake City, Utah, USA*
[2] *The Graduate School of Science and Engineering, Saitama University, Saitama, Saitama, Japan*
[3] *Graduate School of Science and Engineering, Tokyo Institute of Technology, Meguro, Tokyo, Japan*
[4] *Department of Physics and The Research Institute of Natural Science, Hanyang University, Seongdong-gu, Seoul, Korea*
[5] *Department of Physics, Tokyo University of Science, Noda, Chiba, Japan*
[6] *Department of Physics, Kindai University, Higashi Osaka, Osaka, Japan*
[7] *Service de Physique Théorique, Université Libre de Bruxelles, Brussels, Belgium*
[8] *The Hakubi Center for Advanced Research and Graduate School of Science, Kyoto University, Kitashirakawa-Oiwakecho, Sakyo-ku, Kyoto, Japan*
[9] *Institute for Cosmic Ray Research, University of Tokyo, Kashiwa, Chiba, Japan*
[10] *Graduate School of Science, Osaka City University, Osaka, Osaka, Japan*
[11] *Kavli Institute for the Physics and Mathematics of the Universe (WPI), Todai Institutes for Advanced Study, University of Tokyo, Kashiwa, Chiba, Japan*
[12] *Information Engineering Graduate School of Science and Technology, Shinshu University, Nagano, Nagano, Japan*
[13] *Faculty of Engineering, Kanagawa University, Yokohama, Kanagawa, Japan*
[14] *Interdisciplinary Graduate School of Medicine and Engineering, University of Yamanashi, Kofu, Yamanashi, Japan*
[15] *Earthquake Research Institute, University of Tokyo, Bunkyo-ku, Tokyo, Japan*
[16] *Academic Assembly School of Science and Technology Institute of Engineering, Shinshu University, Nagano, Nagano, Japan*
[17] *Astrophysical Big Bang Laboratory, RIKEN, Wako, Saitama, Japan*
[18] *Department of Physics, Sungkyunkwan University, Jang-an-gu, Suwon, Korea*
[19] *Department of Physics, Tokyo City University, Setagaya-ku, Tokyo, Japan*
[20] *Institute for Nuclear Research of the Russian Academy of Sciences, Moscow, Russia*
[21] *Faculty of Systems Engineering and Science, Shibaura Institute of Technology, Minato-ku, Tokyo, Japan*
[22] *Department of Engineering Science, Faculty of Engineering, Osaka Electro-Communication University, Neyagawa-shi, Osaka, Japan*
[23] *Department of Physics, Chiba University, Chiba, Chiba, Japan*
[24] *Department of Physics, Yonsei University, Seodaemun-gu, Seoul, Korea*
[25] *Faculty of Science, Kochi University, Kochi, Kochi, Japan*
[26] *Nambu Yoichiro Institute of Theoretical and Experimental Physics, Osaka City University, Osaka, Osaka, Japan*
[27] *Department of Physical Sciences, Ritsumeikan University, Kusatsu, Shiga, Japan*
[28] *Advanced Research Institute for Science and Engineering, Waseda University, Shinjuku-ku, Tokyo, Japan*
[29] *Sternberg Astronomical Institute, Moscow M.V. Lomonosov State University, Moscow, Russia*
[30] *Department of Physics, School of Natural Sciences, Ulsan National Institute of Science and Technology, UNIST-gil, Ulsan, Korea*
[31] *Department of Physics and Astronomy, Rutgers University - The State University of New Jersey, Piscataway, New Jersey, USA*
[32] *Graduate School of Information Sciences, Hiroshima City University, Hiroshima, Hiroshima, Japan*
[33] *Institute of Particle and Nuclear Studies, KEK, Tsukuba, Ibaraki, Japan*
[34] *National Institute of Radiological Science, Chiba, Chiba, Japan*
[35] *CEICO, Institute of Physics, Czech Academy of Sciences, Prague, Czech Republic*
[36] *Department of Physics and Institute for the Early Universe, Ewha Womans University, Seodaemun-gu, Seoul, Korea*
[37] *Department of Physics, Ehime University, Matsuyama, Ehime, Japan*

145 members, 32 institutes, 7 countries

Russia

Belgium

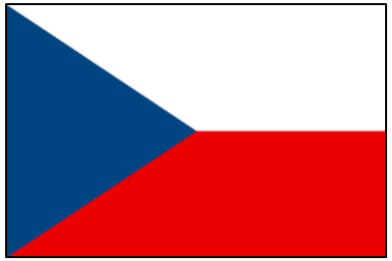

Czech Republic

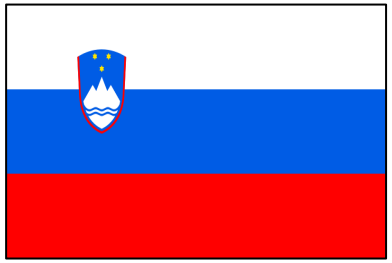

Slovenia

Telescope Array (TA) experiment

- The largest cosmic ray observatory in the northern hemisphere

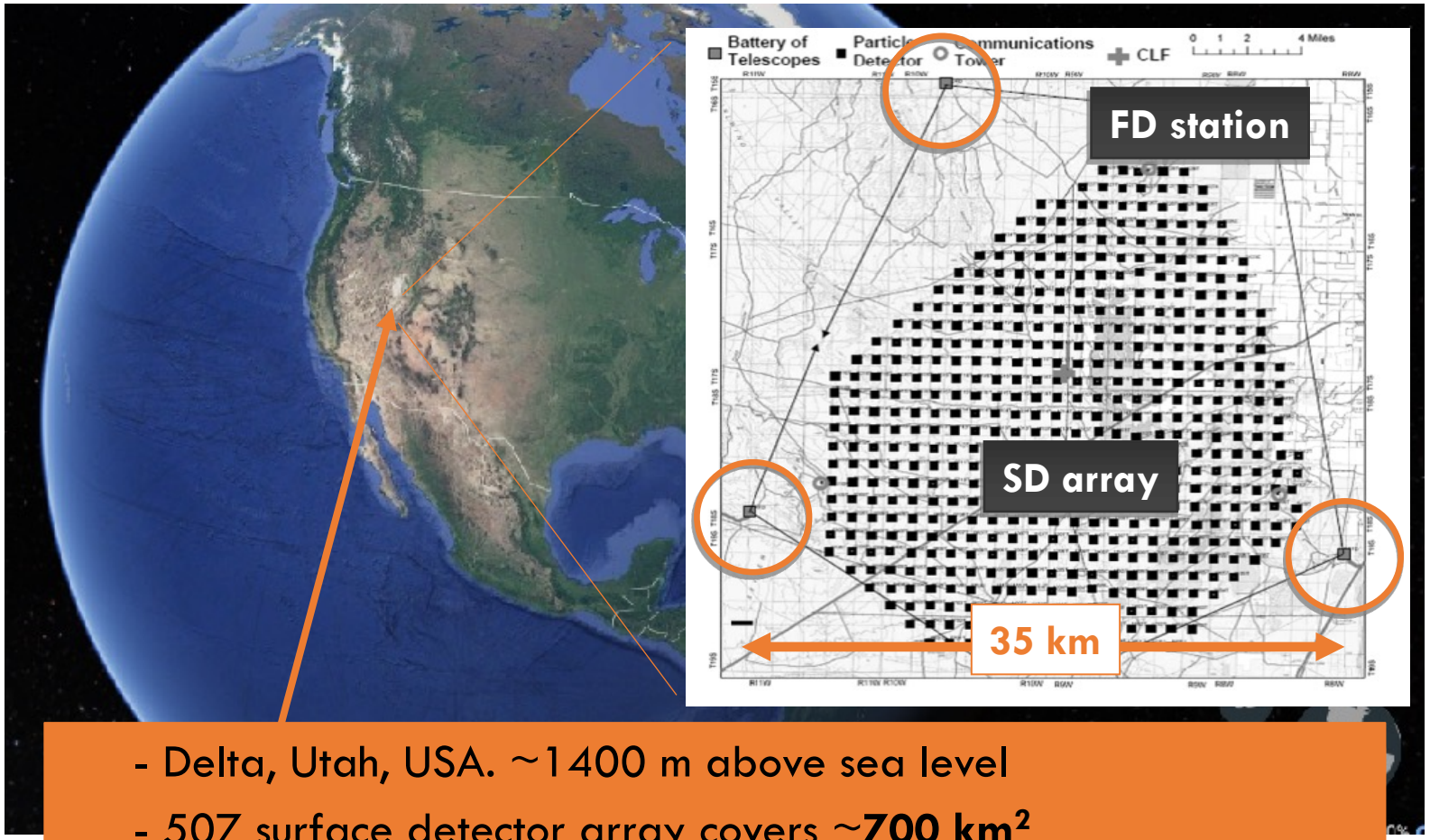

- Delta, Utah, USA. ~1400 m above sea level
- 507 surface detector array covers ~**700 km²**
- 38 telescopes in 3 stations look over the array

Surface Detector: Plastic Scintillator

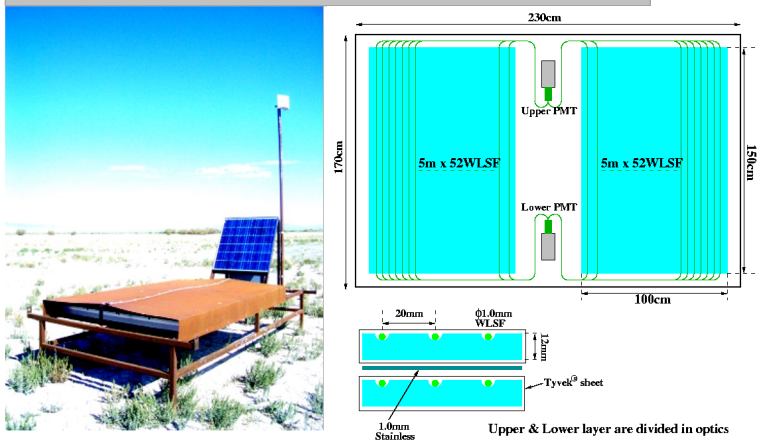

Fluorescence Detector: PMT camera

Anisotropies in the arrival direction distributions of UHECRs

Arrival direction distribution: What are their sources?

- Anisotropy search is critical to narrowing down source candidates of UHECRs.

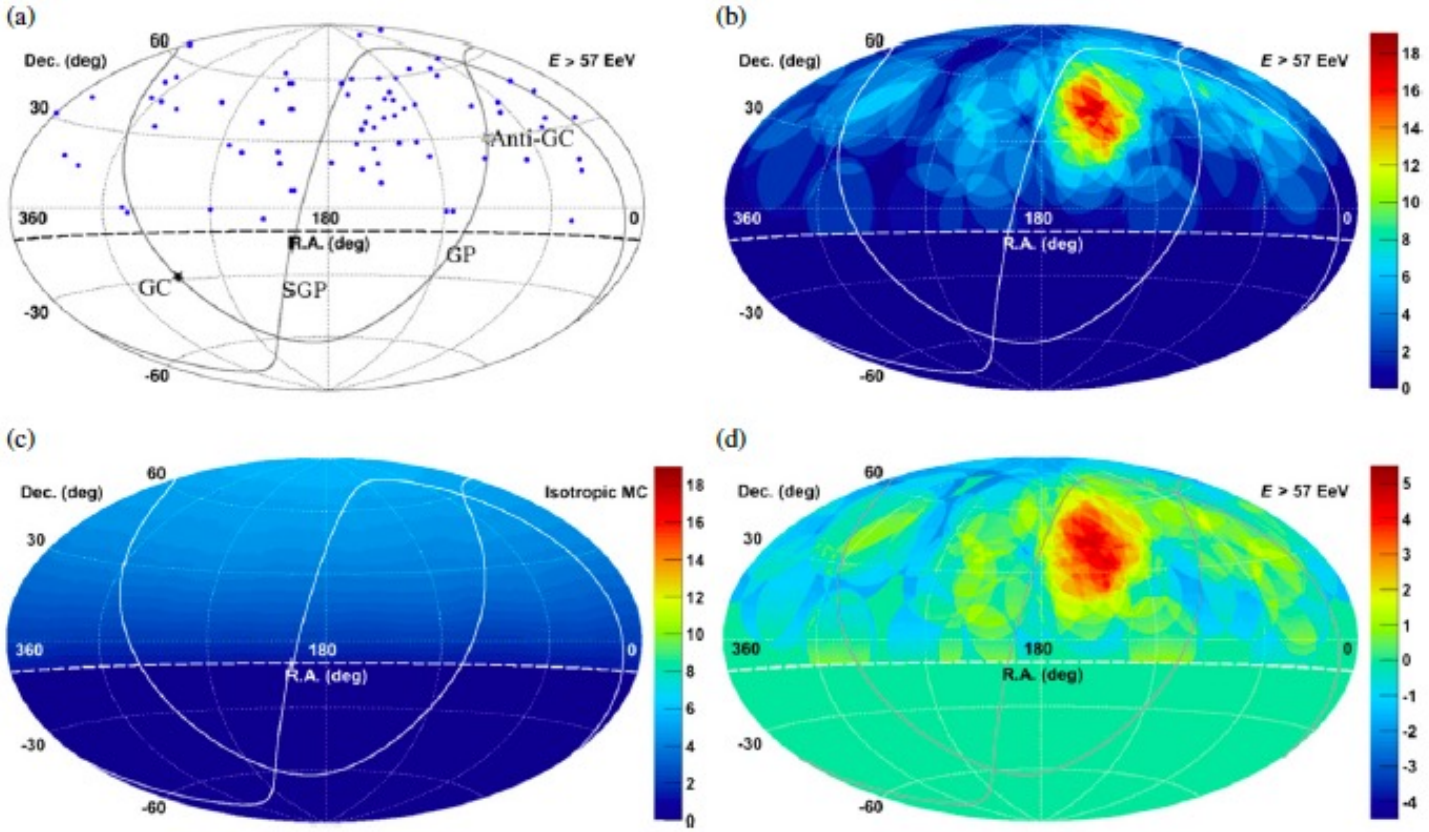

Figure 1. Aitoff projection of the UHECR maps in equatorial coordinates. The solid curves indicate the galactic plane (GP) and supergalactic plane (SGP). Our FoV is defined as the region above the dashed curve at decl. $= -10°$. (a) The points show the directions of the UHECRs $E > 57$ EeV observed by the TA SD array, and the closed and open stars indicate the Galactic center (GC) and the anti-Galactic center (Anti-GC), respectively; (b) color contours show the number of observed cosmic-ray events summed over a 20° radius circle; (c) number of background events from the geometrical exposure summed over a 20° radius circle (the same color scale as (b) is used for comparison); (d) significance map calculated from (b) and (c) using Equation (1).

- We performed **intermediate scale anisotropy** searches.
- 72 events with E > 5.7×10^{19} eV (5-year TA SD data)
- Maximum local significance: 5.1σ
  Observed: 19 events
  Expected from iso.: 4.5 events
- Post-trial probability:

$P(\mathrm{p_{pre}} > 5.1\sigma) = 3.7\times10^{-4}$

→ 3.4σ

TA Collab. (2014)

Oversampling Searches: Li-Ma Method

- The statistical significance of the excess of events compared to background events at each grid point is calculated by the Li-Ma method:

$$S_{\mathrm{LM}} = \sqrt{2}\left[N_{\mathrm{on}} \ln\left(\frac{(1+\alpha)N_{\mathrm{on}}}{\alpha(N_{\mathrm{on}}+N_{\mathrm{off}})}\right) + N_{\mathrm{off}} \ln\left(\frac{(1+\alpha)N_{\mathrm{off}}}{N_{\mathrm{on}}+N_{\mathrm{off}}}\right)\right]^{1/2},$$

  - $N_{\mathrm{total}} = N_{\mathrm{on}} + N_{\mathrm{off}}$: total observed number of events
  - N_{on}: # of events inside the circle, N_{off}: # of events outside the circle
  - $N_{\mathrm{bg}} = \alpha \cdot N_{\mathrm{off}}$

- To determine the exposure ratio of α, we generated 10^5 events assuming an isotropic flux taking into account the geometrical exposure.
  - $\alpha = \frac{N_{\mathrm{sim,on}}}{N_{\mathrm{sim,off}}} = \frac{N_{\mathrm{sim,circle}}}{(N_{\mathrm{sim,total}} - N_{\mathrm{sim,circle}})}$
- Field of view: 90° to -10° in declination, 0° to 360° in right ascension
- Oversampling with **25°** of angular windows

Li-Ma Significance Map with E ≥ 57 EeV

25°-radius oversampling

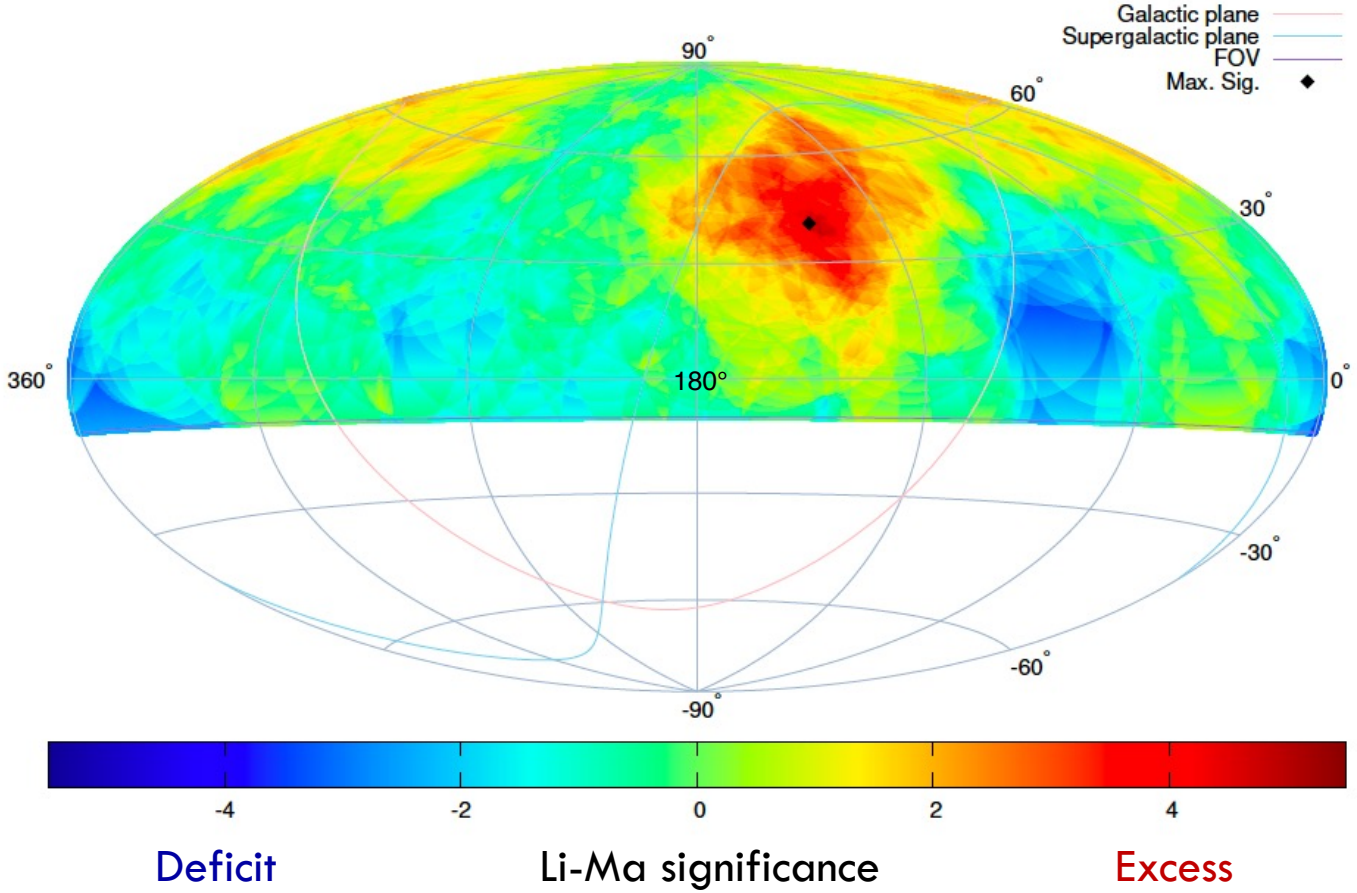

- 205 events (14-year TA SD data)
- Max local sig.: **5.1σ** at (144.0°, 40.5°)

  Obs. : 44 events
  N_{bg} : 16.9 events
  } ~160% excess
- Post-trial probability:

$$P(S_{MC} > 5.1\sigma) = 7.4\times10^{-4} \rightarrow \mathbf{3.2\sigma}$$

Independent Dataset Analysis

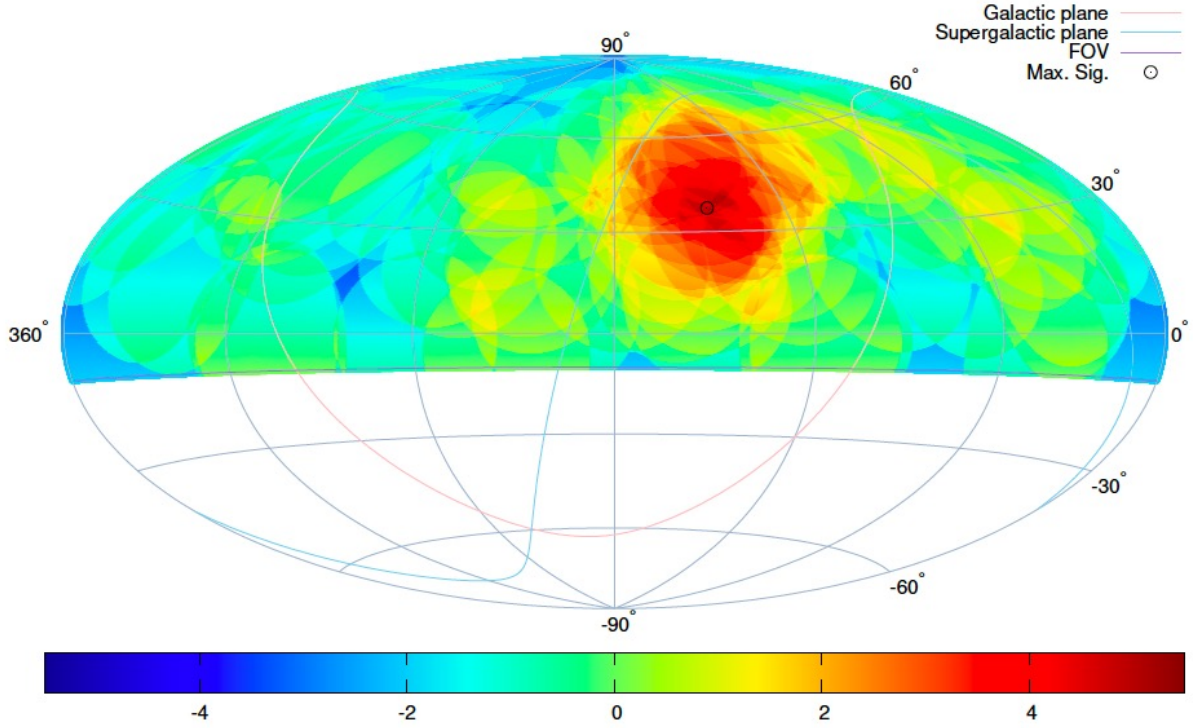

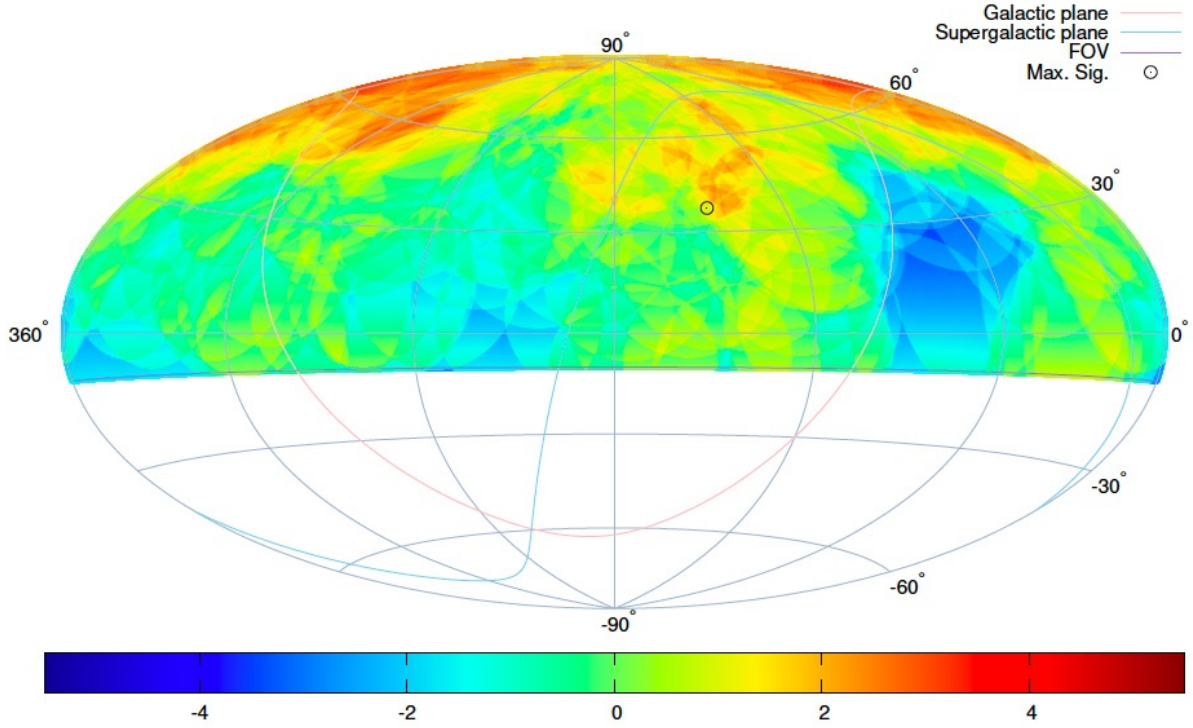

- 72 events (First 5-year)
- **5.0σ** at (144.0°, 40.5°)
  Obs. : 22 events
  N_{bg} : 5.2 events

- 133 events (Last 9-year)
- **2.5σ** at (144.0°, 40.5°)
  Obs. : 22 events
  N_{bg} : 11.6 events

Growth of the Hotspot

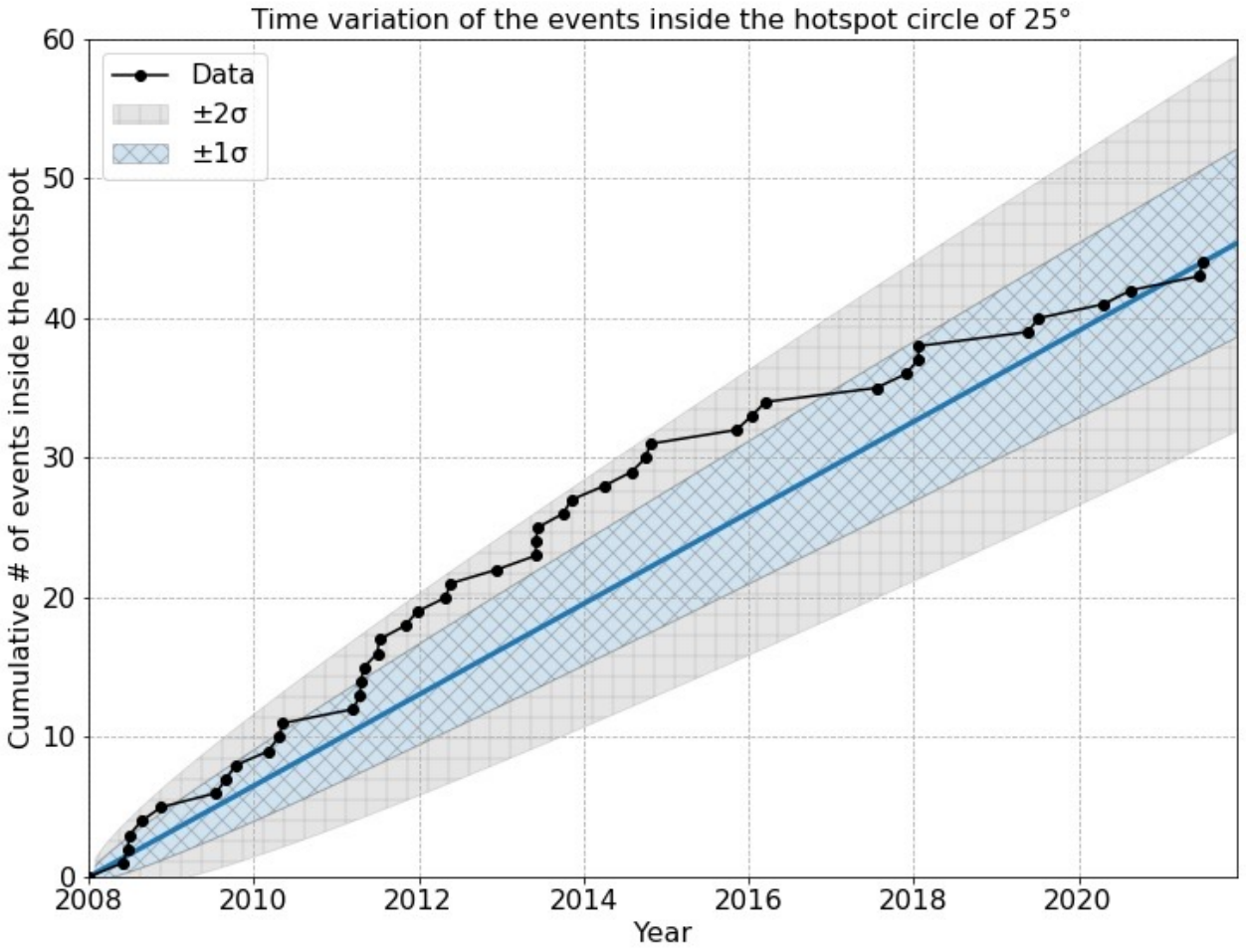

- Black dots: cumulative # of events falling inside the hotspot circle of 25°

- Blue solid line: estimated event rate inside the hotspot

The increase rate of the events inside the hotspot circle is **consistent with the linear increase within ~2σ.**

Event Ratio of the Hotspot

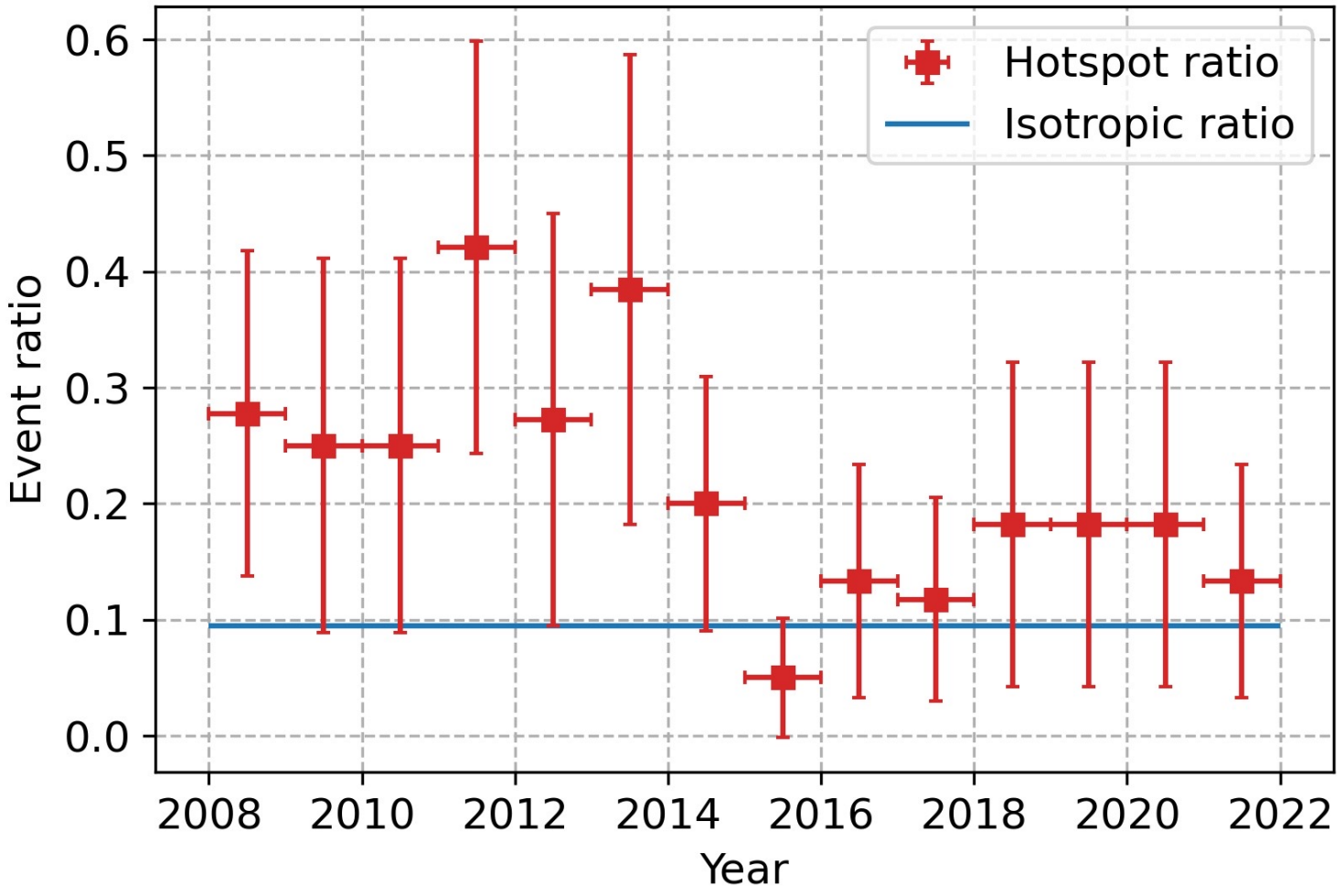

Hotspot ratio:

# of events inside the hotspot/total # of events

Isotropic ratio (Hotspot aperture):

# of isotropic simulation events inside the hotspot / total # of isotropic simulation events (10^5)

(different from the definition of α)

$$\beta = \frac{N_{\mathrm{sim,circle}}}{N_{\mathrm{sim,total}}}$$

$$\alpha = \frac{N_{\mathrm{sim,on}}}{N_{\mathrm{sim,off}}} = \frac{N_{\mathrm{sim,circle}}}{(N_{\mathrm{sim,total}} - N_{\mathrm{sim,circle}})}$$

This plot shows that we observed more events inside the hotspot compared to the isotropic expectation except for one year.

New excess in the direction of the Perseus-Pisces supercluster

Excesses in the energy spectrum

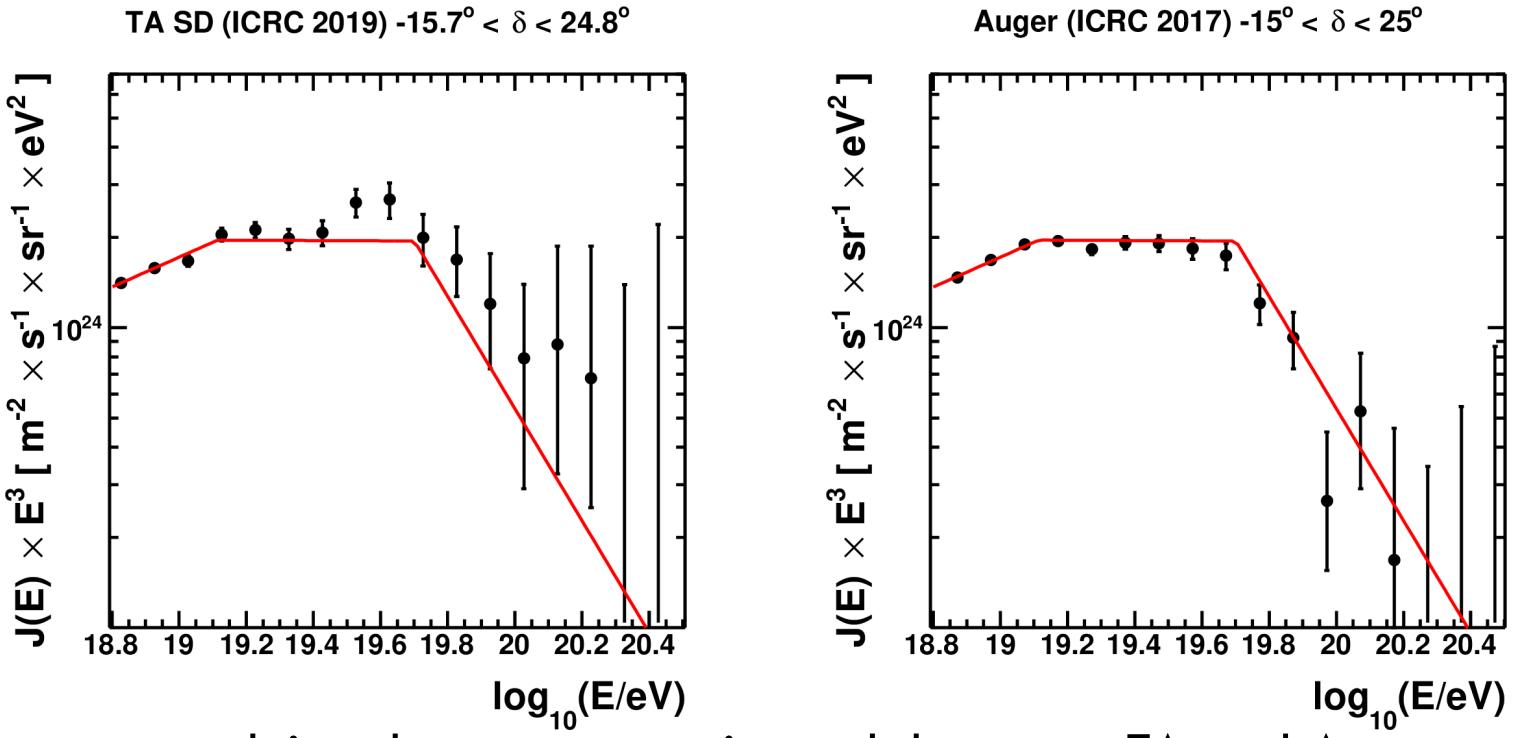

- While we were studying the spectrum mismatch between TA and Auger, we made sky maps of events for energy ranges, $E \geq 10^{19.4}$ eV, $E \geq 10^{19.5}$ eV, and $E \geq 10^{19.6}$ eV, since we were investigating whether the hotspot extends down into lower declinations at slightly lower energies.
- The maximum Li-Ma significance appeared at the location of the Perseus-Pisces supercluster for each energy range.

Oversampling Searches: Li-Ma Method

- The statistical significance of the excess of events compared to background events at each grid point is calculated by the Li-Ma method:

$$S_{\mathrm{LM}} = \sqrt{2}\left[N_{\mathrm{on}} \ln\left(\frac{(1+\alpha)N_{\mathrm{on}}}{\alpha(N_{\mathrm{on}}+N_{\mathrm{off}})}\right) + N_{\mathrm{off}} \ln\left(\frac{(1+\alpha)N_{\mathrm{off}}}{N_{\mathrm{on}}+N_{\mathrm{off}}}\right)\right]^{1/2},$$

  - $N_{\mathrm{total}} = N_{\mathrm{on}} + N_{\mathrm{off}}$: total observed number of events
  - N_{on}: # of events inside the circle, N_{off}: # of events outside the circle
  - $N_{\mathrm{bg}} = \alpha \cdot N_{\mathrm{off}}$

- To determine the exposure ratio of α, we generated 10^5 events assuming an isotropic flux taking into account the geometrical exposure.
  - $\alpha = \frac{N_{\mathrm{sim,on}}}{N_{\mathrm{sim,off}}} = \frac{N_{\mathrm{sim,circle}}}{(N_{\mathrm{sim,total}} - N_{\mathrm{sim,circle}})}$
- Field of view: 90° to -15.7° in declination, 0° to 360° in right ascension
- Oversampling with **20°** of angular windows

New excess in Slightly Lower Energy Events TA Collab., ICRC2021

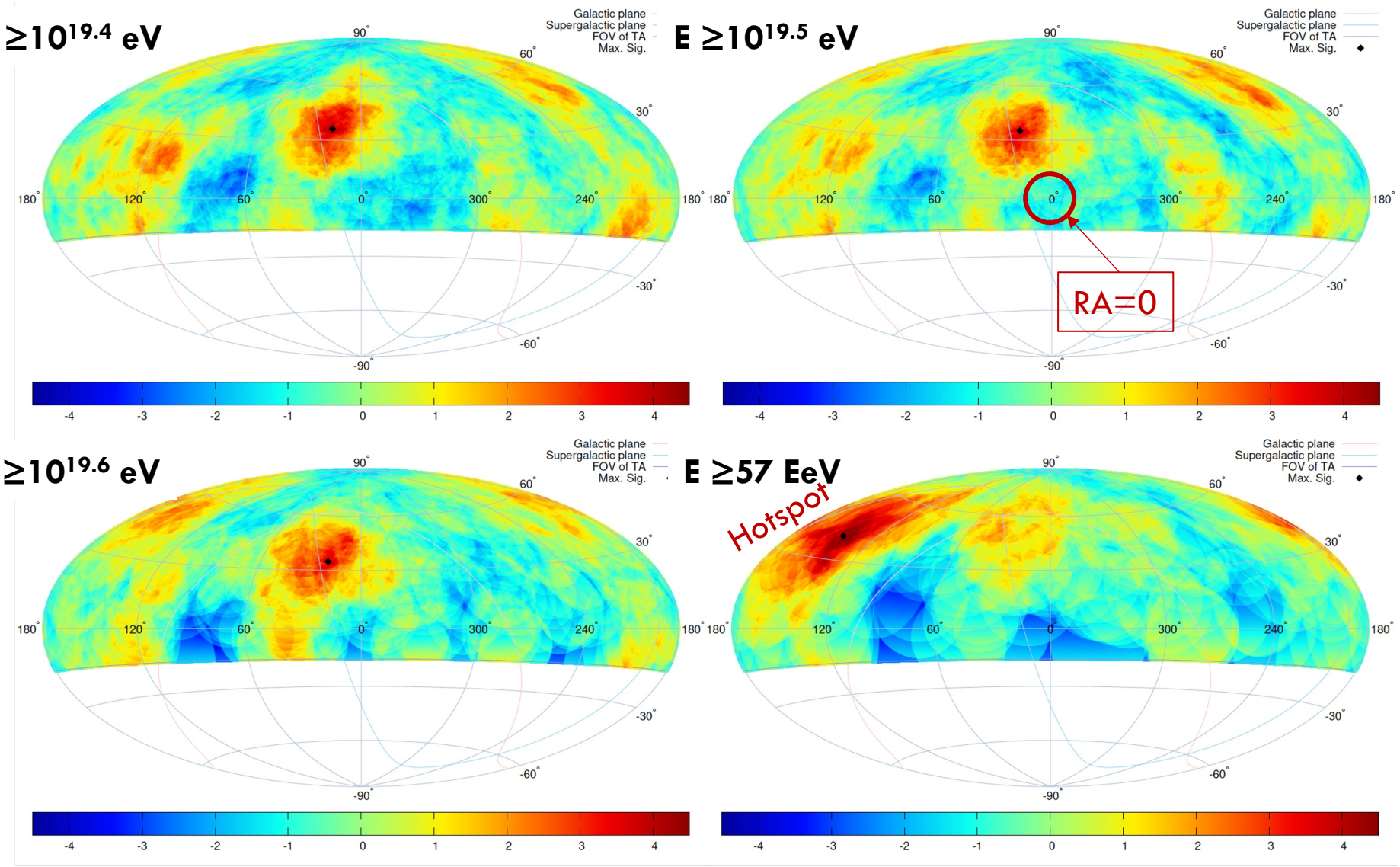

- Li-Ma significance map: excess (red) / deficit (blue) of events compared to isotropy
- Black diamond (◆): the maximum Li-Ma significance position
- Equatorial coords. having RA=0 at center

Li-Ma Significance Map with $E \geq 10^{19.4}$ eV

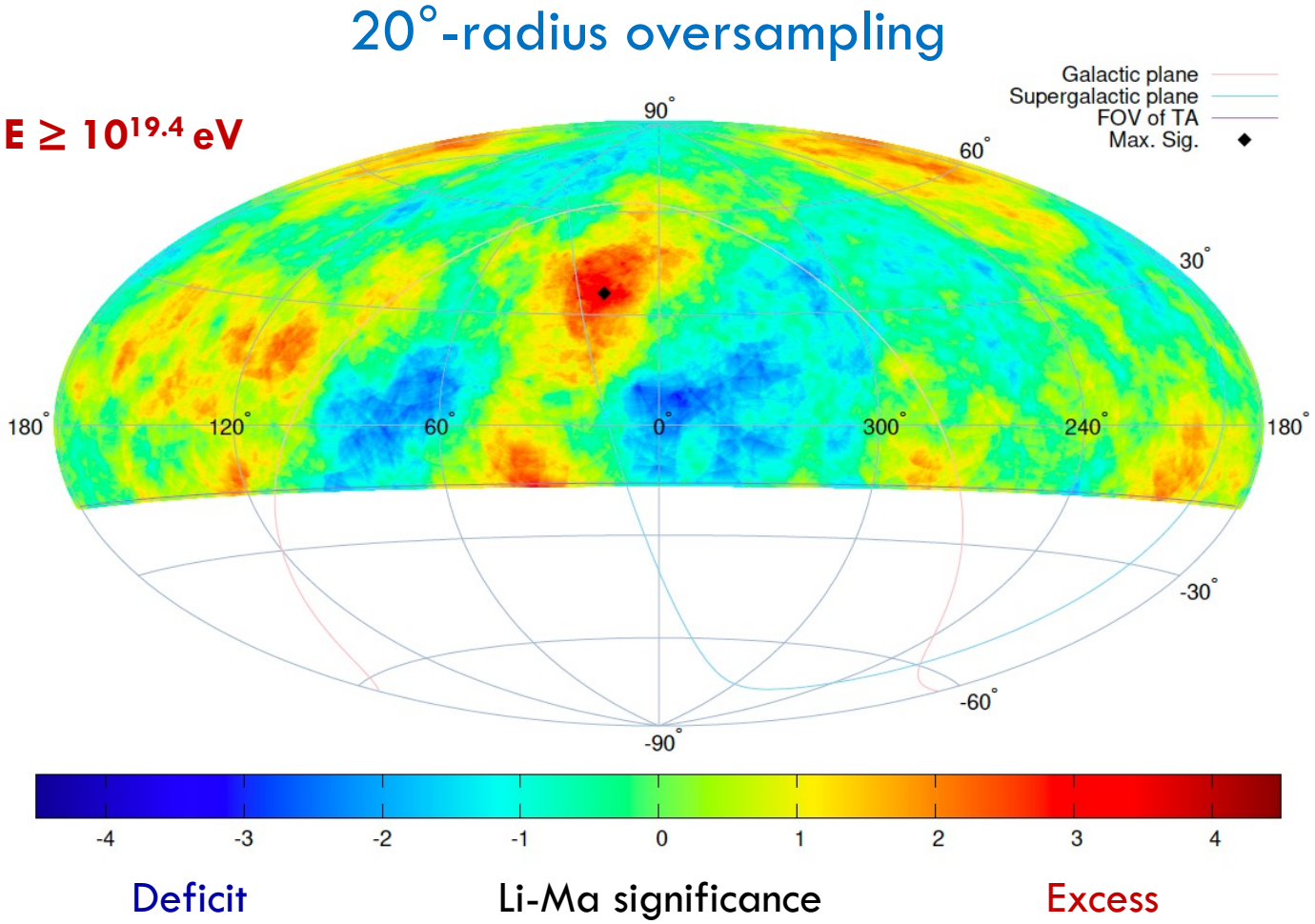

- 1060 events (14-year TA SD data)

- Li-Ma sig.: 3.8σ at (17.4°, 36.0°)

  Obs.: 95 events

  N_{bg}: 61.4 events

  } ~55% excess

Li-Ma Significance Map with $E \geq 10^{19.5}$ eV

20°-radius oversampling

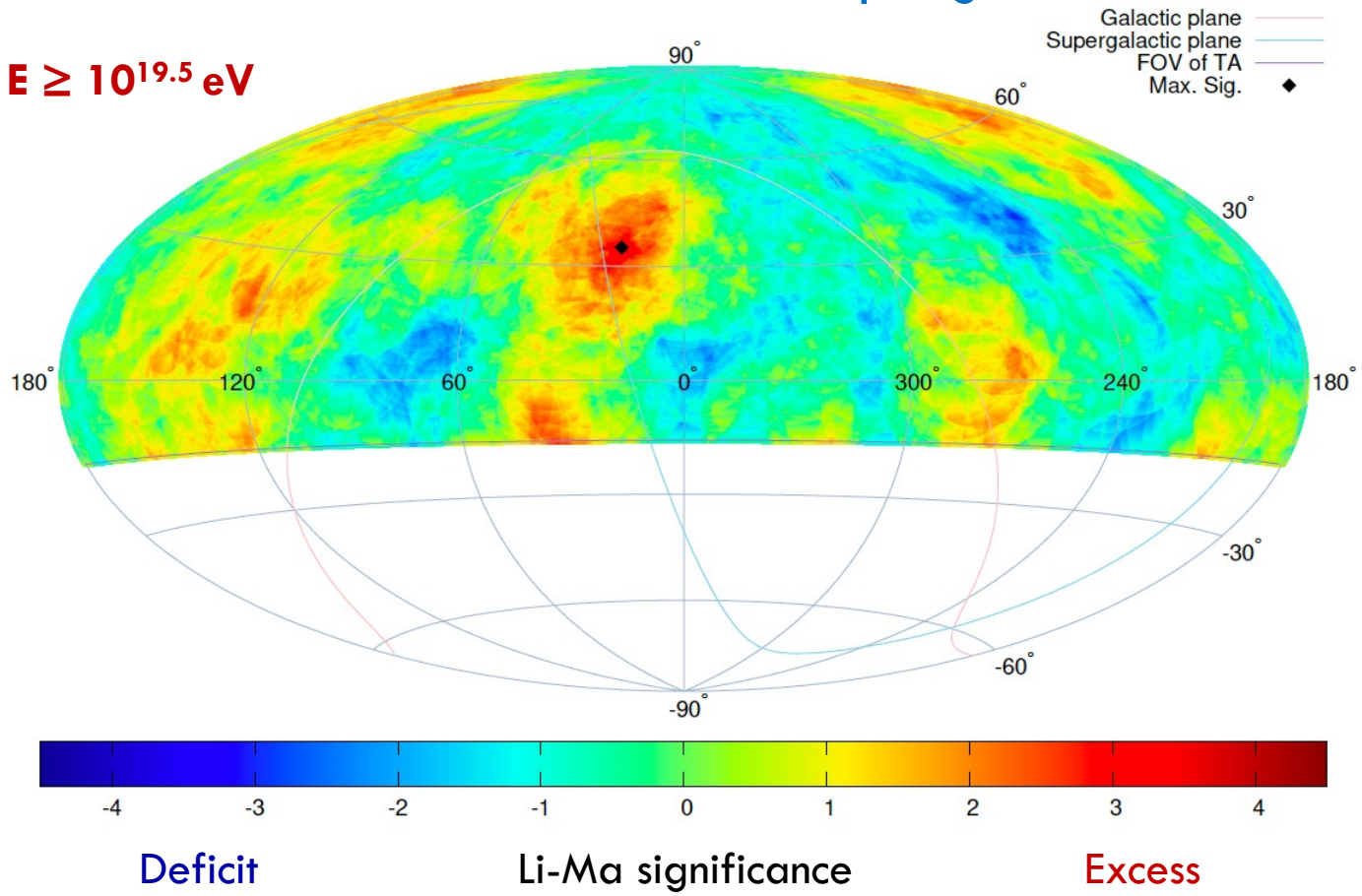

- 685 events (14-year TA SD data)

- Li-Ma sig.: 3.8σ at (19.0°, 35.1°)

  Obs.: 66 events

  N_{bg}: 39.1 events

  } ~69% excess

Li-Ma Significance Map with $E \geq 10^{19.6}$ eV

20°-radius oversampling

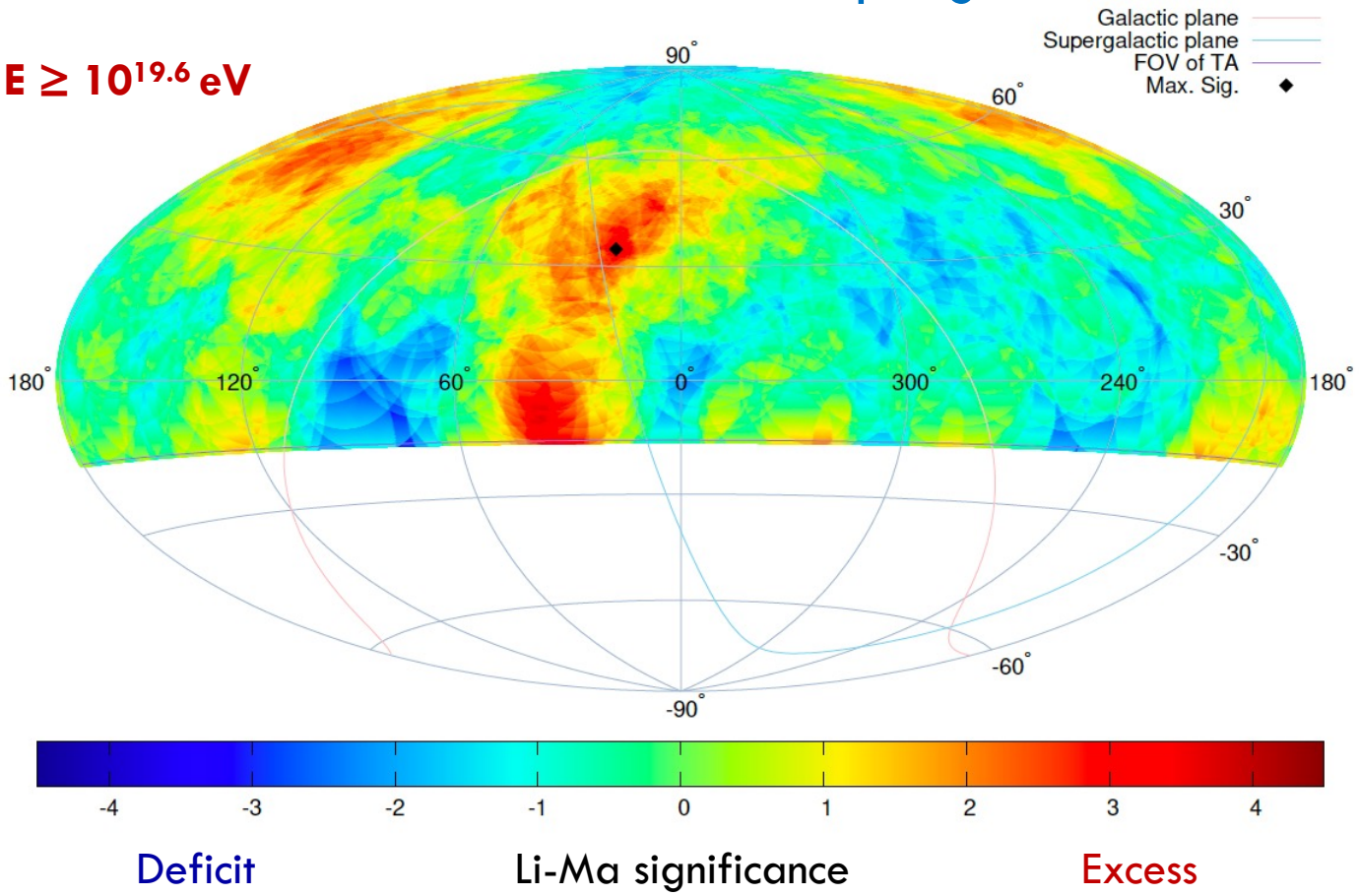

- 413 events (14-year TA SD data)

- Li-Ma sig.: 3.5σ at (19.7°, 34.6°)

  Obs.: 43 events

  N_{bg}: 23.2 events

  } ~85% excess

What is Behind the New Excess?

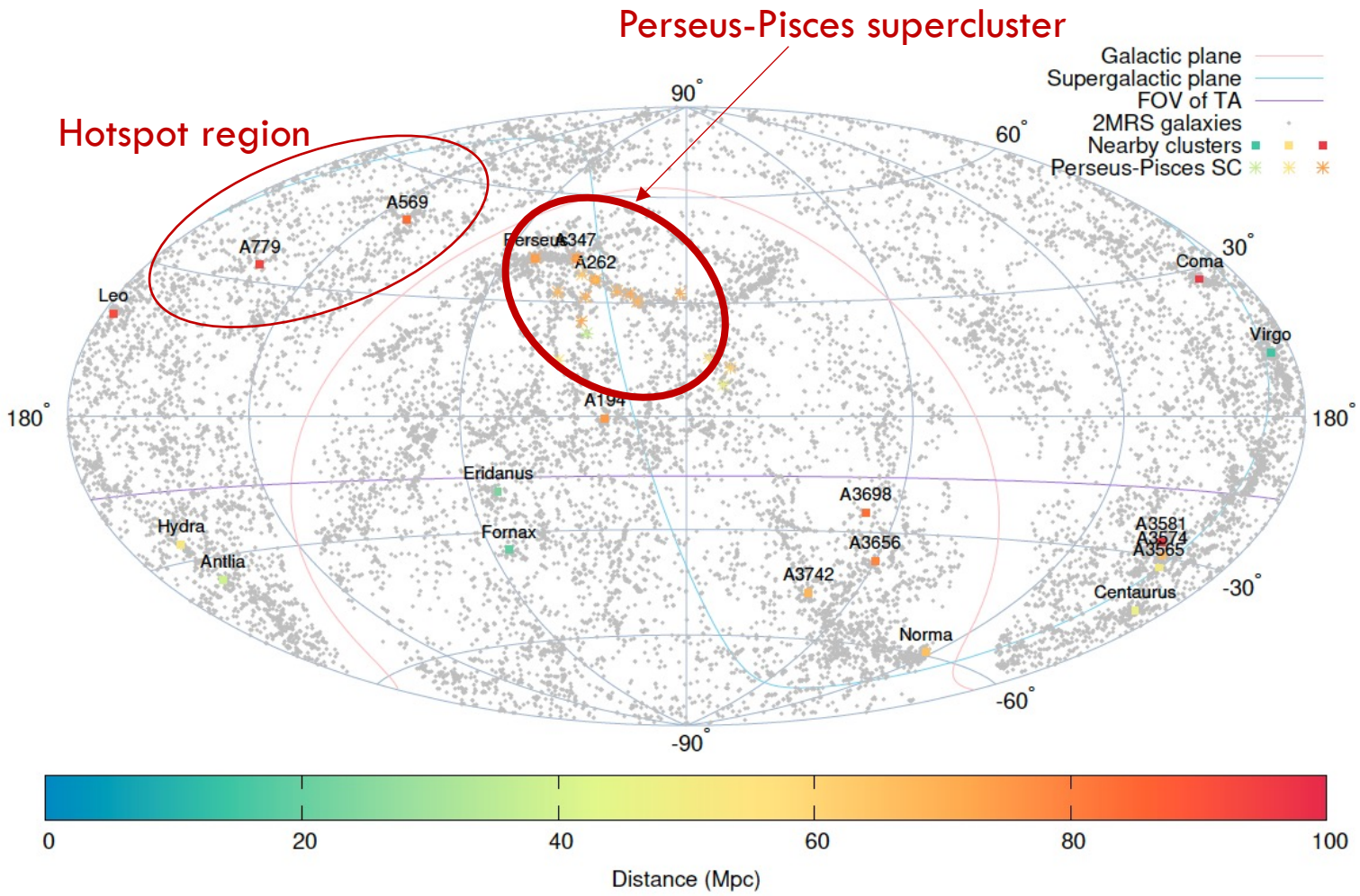

Sky map with nearby galaxies and clusters of galaxies in equatorial coordinates

- Gray dots (·): nearby galaxies from the 2MASS Redshift Survey catalog
- Colored squares (■): nearby clusters of galaxies
- Colored asterisks (*): representative elements of Perseus-Pisces supercluster

Equatorial coordinates

Characteristic of the Perseus-Pisces Supercluster (PPSC)

3-dimensional density maps

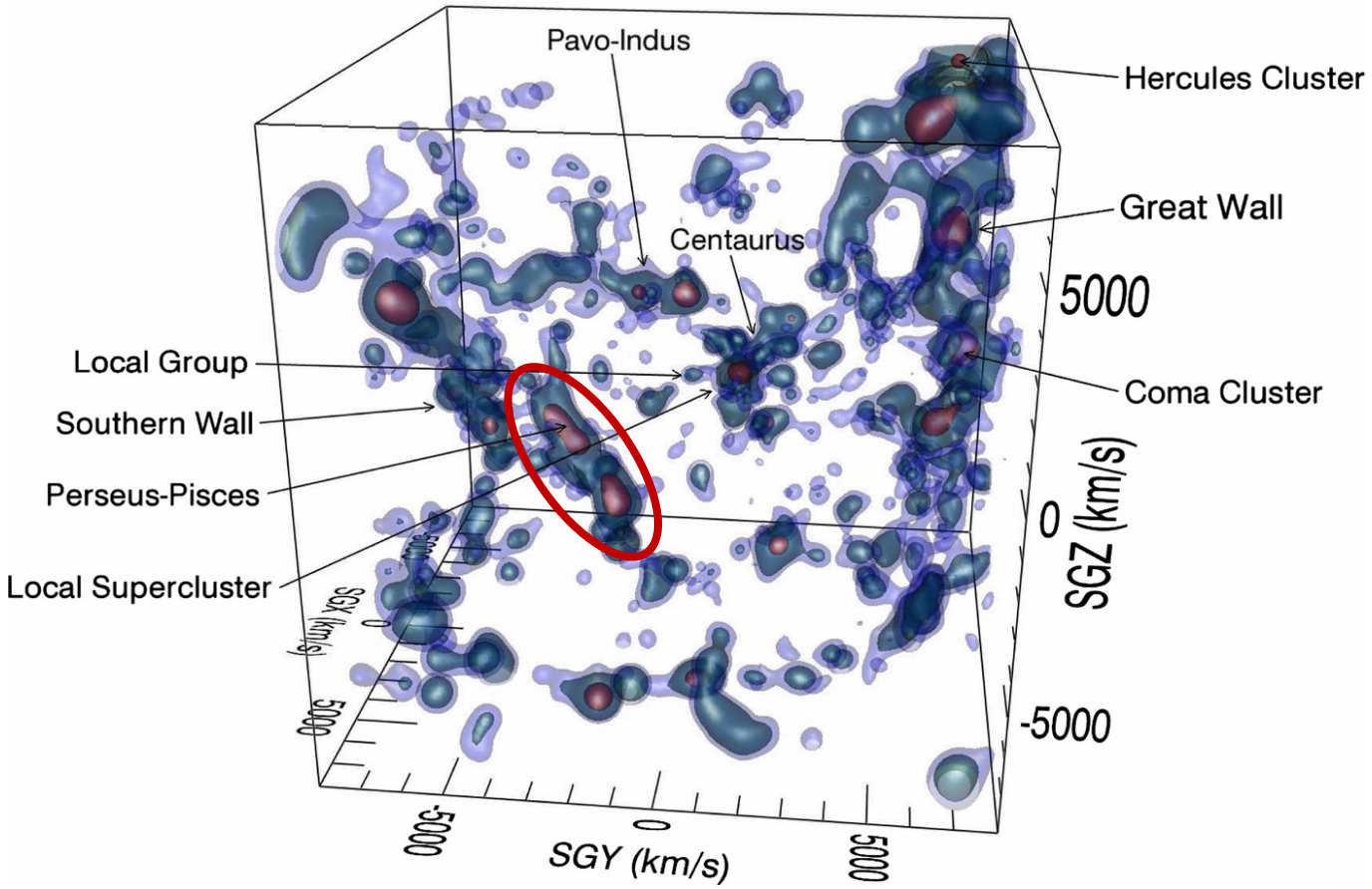

Courtois *et al.* (2013)

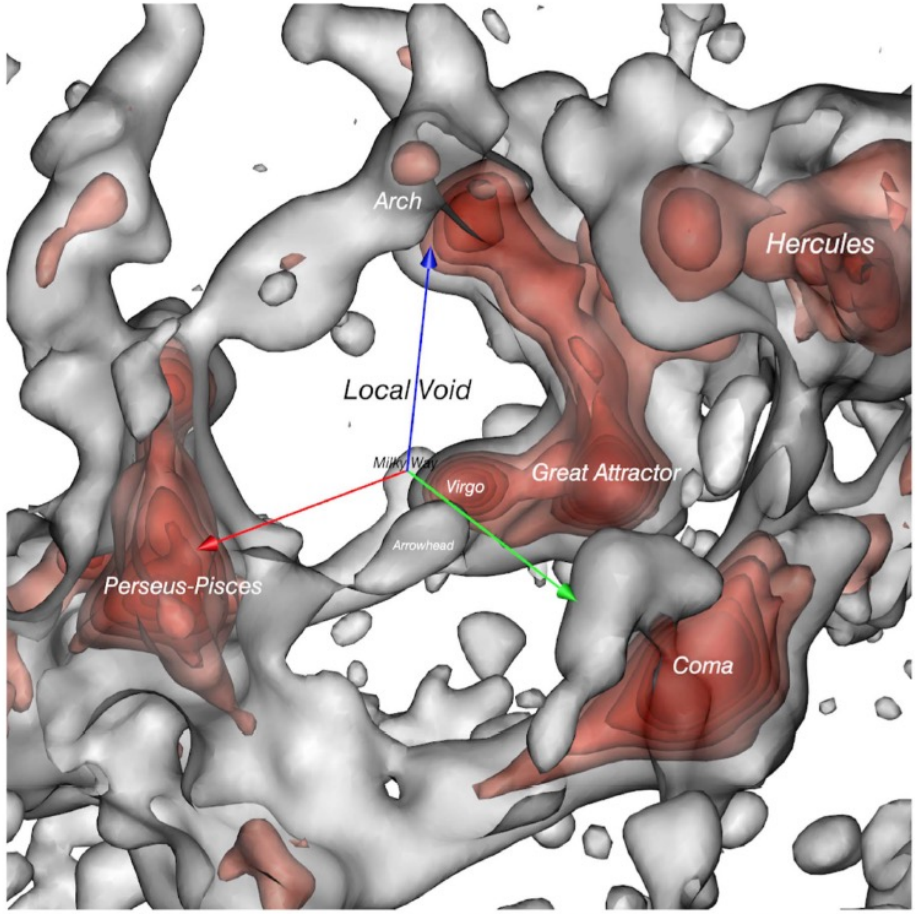

Tully *et al.* (2019)

PPSC Excess and representative elements of PPSC

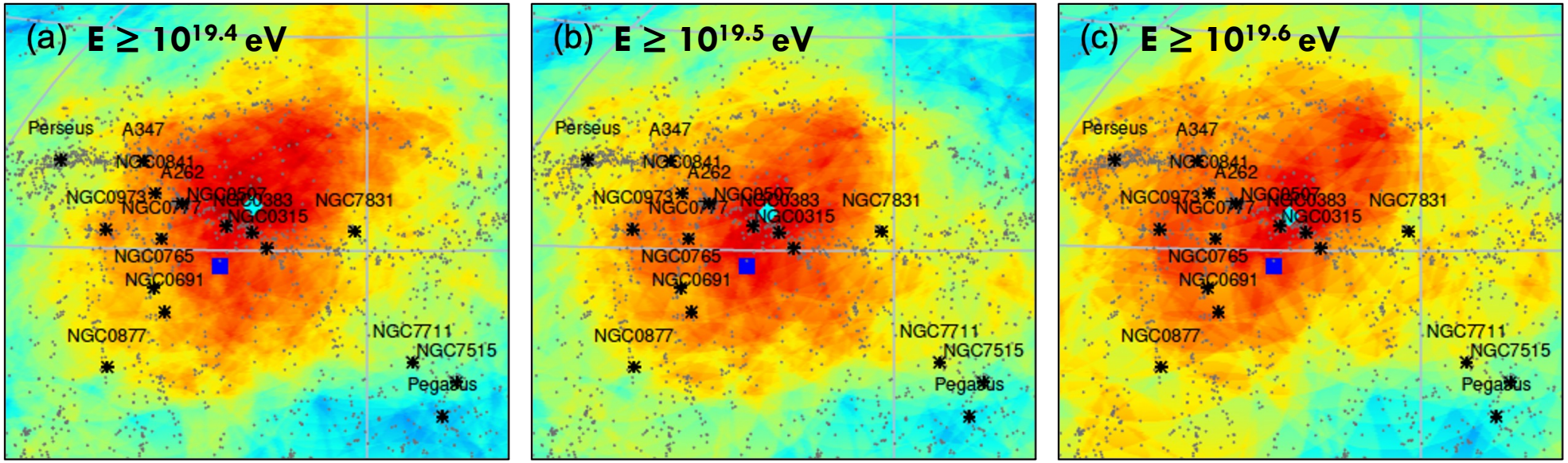

- Black asterisks (*): the representative elements of the PPSC; Gray dots (·): Galaxies from the 2MASS Redshift Survey catalog (35 – 100 Mpc); Cyan diamonds (◆): the positions of maximum excesses; Blue squares (■): the center of the PPSC.
- It is seen that the excess is coincident with the overall distribution of the PPSC. The angular separations between the positions of the maximum excesses and the center of the PPSC are less than ~10°.

Independent Dataset Analysis with $E \geq 10^{19.4}$ eV

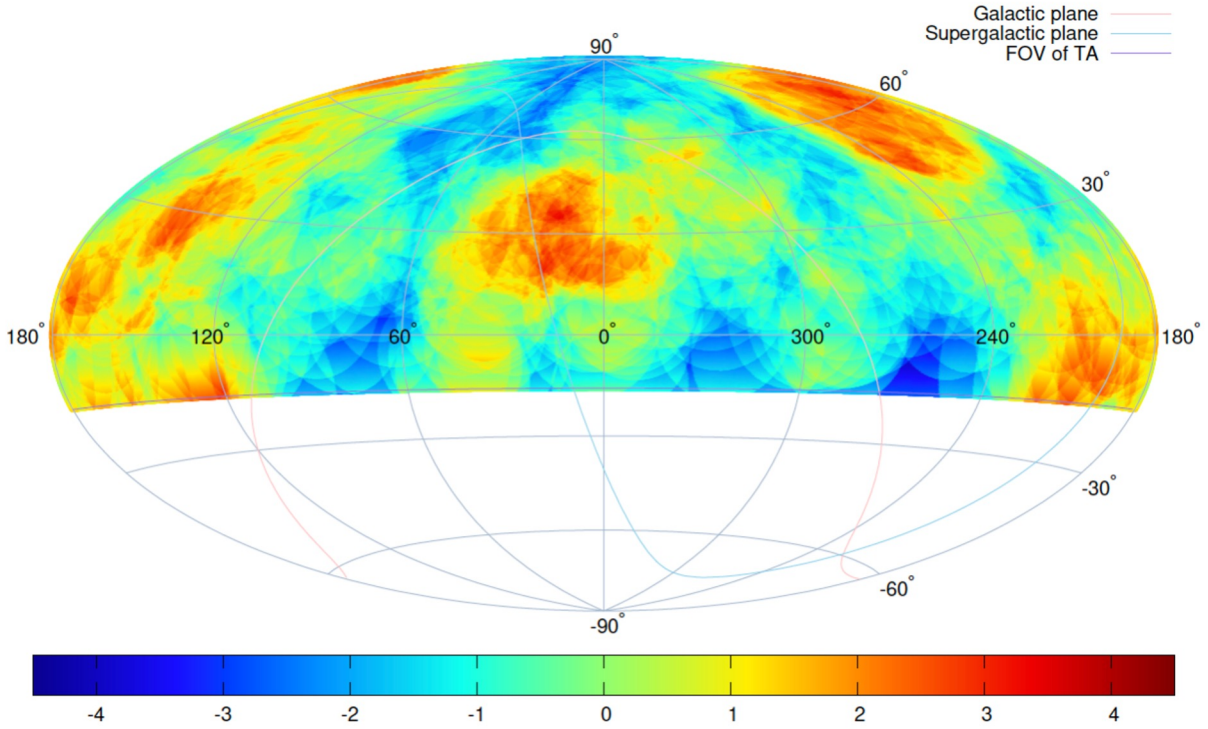

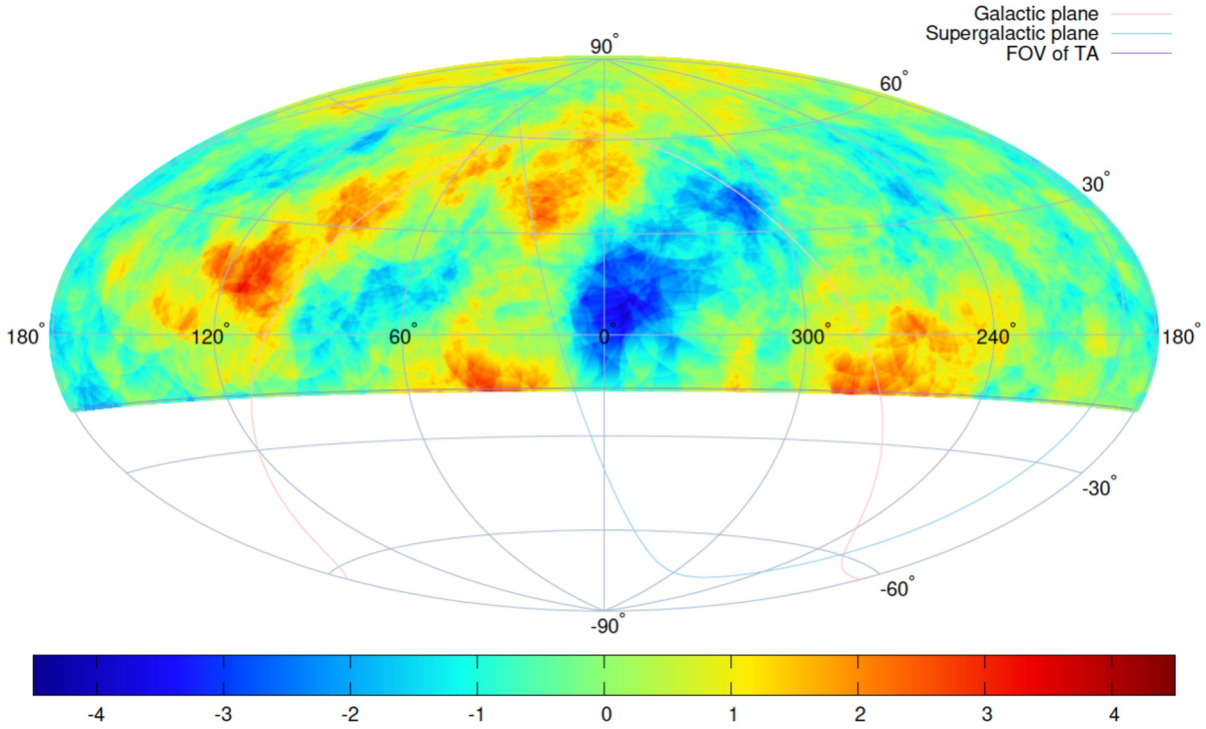

- 389 events (First 5-year)
- **3.3σ** at (17.4°, 36.0°)
  - Obs. : 36 events
  - N_{bg}: 22.4 events

- 671 events (Last 9-year)
- **2.3σ** at (17.4°, 36.0°)
  - Obs. : 55 events
  - N_{bg}: 39.2 events

Growth of the PPSC Excess with E $\geq 10^{19.4}$ eV

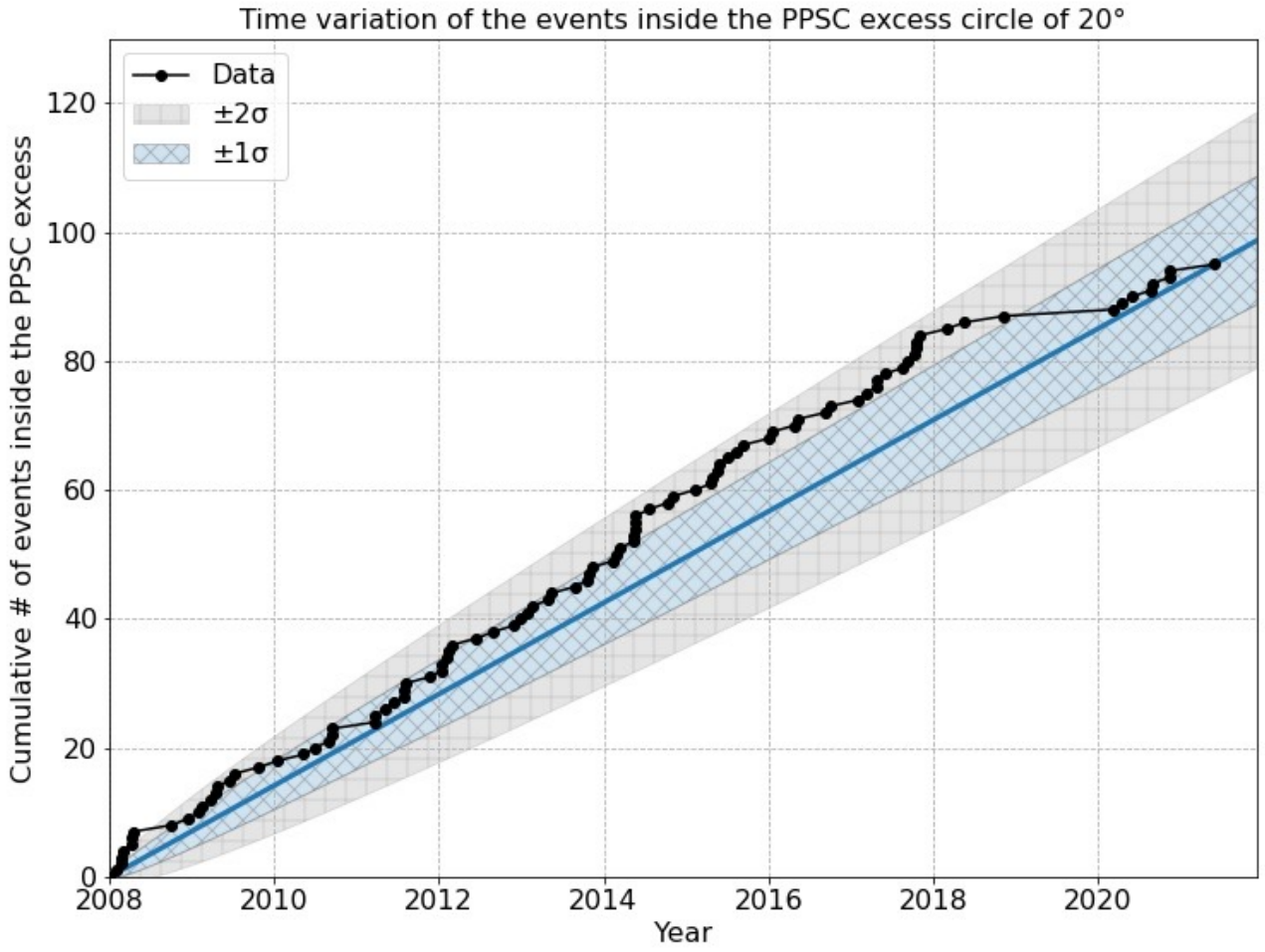

- Black dots: cumulative # of events falling inside the PPSC excess circle of 20°

- Blue solid line: estimated event rate inside the hotspot

The increase rate of the events inside the PPSC excess circle is **consistent with the linear increase within ~2σ.**

Event Ratio of the PPSC Excess

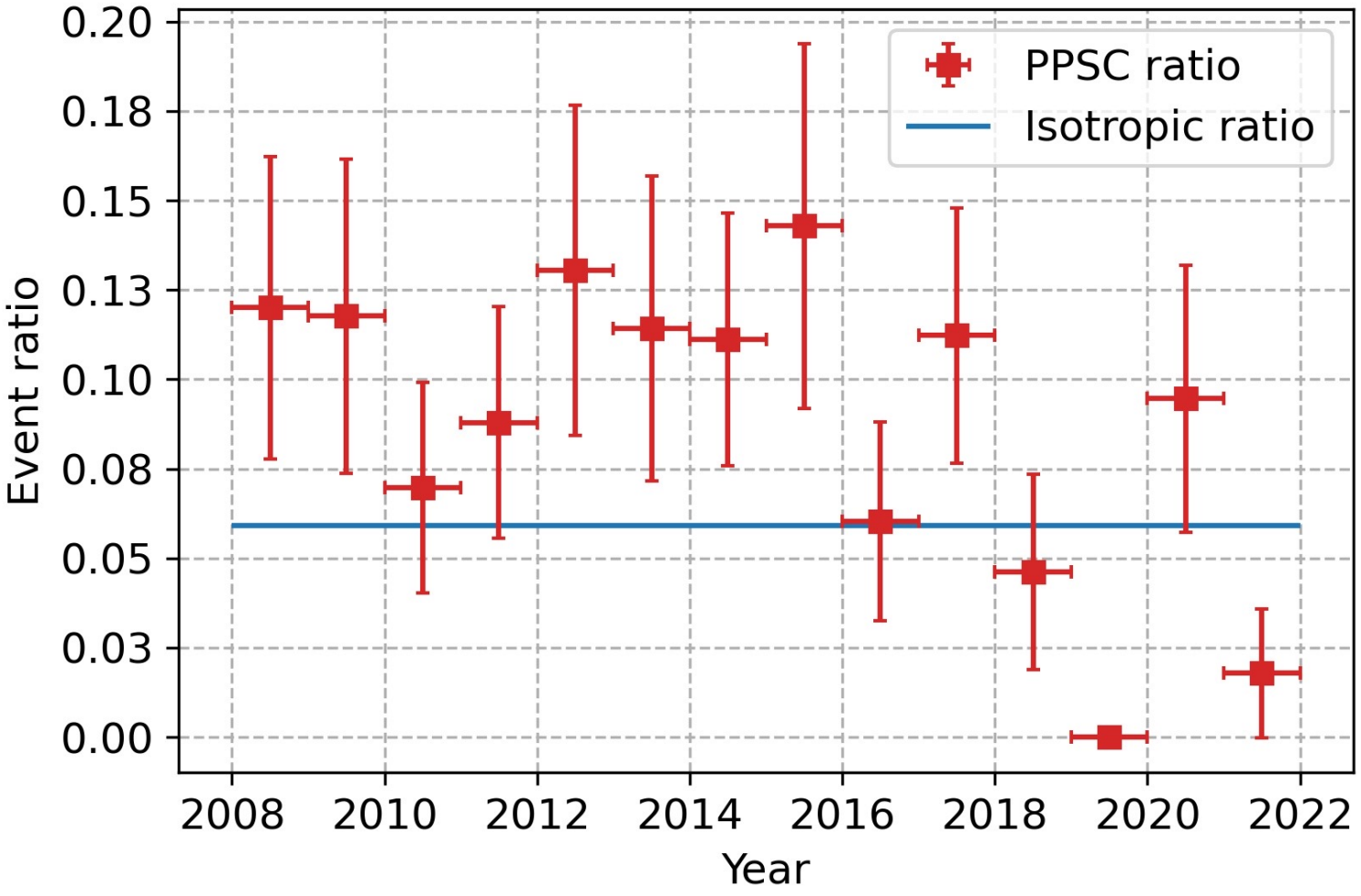

PPSC excess ratio:

# of events inside the PPSC/total # of events

Isotropic ratio (PPSC aperture):

# of isotropic simulation events inside the PPSC / total # of isotropic simulation events (10^5)

(different from the definition of α)

$$\beta = \frac{N_{\mathrm{sim,circle}}}{N_{\mathrm{sim,total}}}$$

$$\alpha = \frac{N_{\mathrm{sim,on}}}{N_{\mathrm{sim,off}}} = \frac{N_{\mathrm{sim,circle}}}{(N_{\mathrm{sim,total}} - N_{\mathrm{sim,circle}})}$$

There are yearly variations, but we have observed higher excess ratios than the isotropic ratio during the most of observation periods.

PPSC Excess and Nearby Major Structures

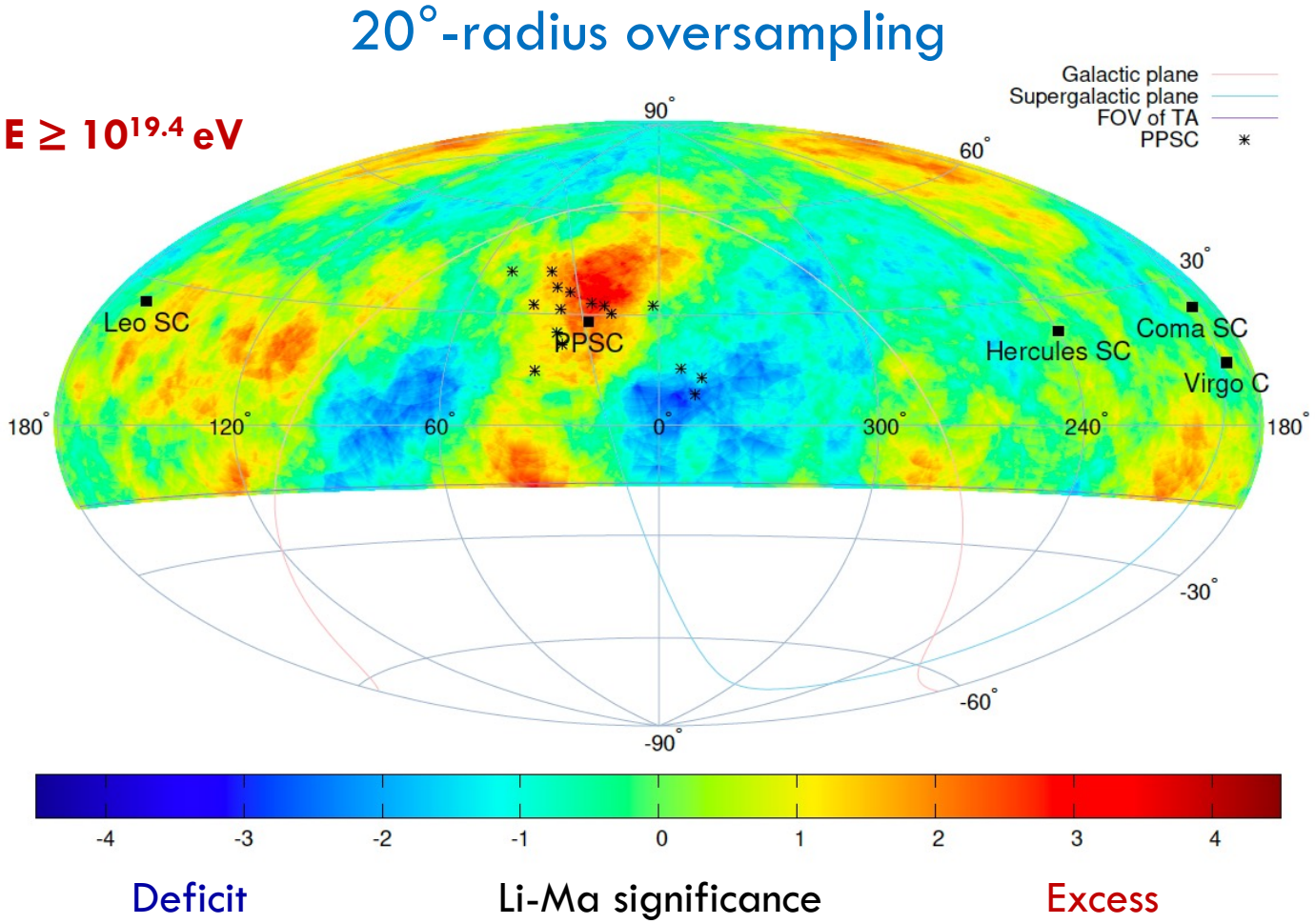

- Choose all the similar major structures to the Perseus-Pisces supercluster in TA's field of view within 150 Mpc.

- Virgo cluster (17 Mpc)
  PPSC (70 Mpc),
  Coma supercluster (90 Mpc)
  Leo supercluster (135 Mpc)
  Hercules supercluster (135 Mpc)

Chance Probability Estimation

- To quantify how often this happens by chance, we generate many Monte-Carlo event sets, each containing the same number of events as the data, thrown isotropically according to the acceptance of the TA SD.
- We count as successes the number of sets where the point of maximum Li-Ma significance is at least as significant as in the data, and also occurs at least as close to the PPSC as in the data: $(S_{mc} \geq S_{obs})$ and $(\theta_{mc} \leq \theta_{obs})$.
- Chance probability of having equal or higher excess on top of the PPSC / major structures {PPSC, Virgo cluster, Coma SC, Leo SC, Hercules SC}

Summary of the Monte-Carlo studies that estimate the chance probability of having an excess

Energy (eV)	Events	Criteria	PPSC	Major structures
$E \geq 10^{19.4}$	1060	$(S_{mc} \geq 3.8\sigma)$ & $(\theta_{mc} \leq 8.6^{\circ})$	3.1σ	2.5σ
$E \geq 10^{19.5}$	685	$(S_{mc} \geq 3.8\sigma)$ & $(\theta_{mc} \leq 7.4^{\circ})$	3.2σ	2.6σ
$E \geq 10^{19.6}$	413	$(S_{mc} \geq 3.5\sigma)$ & $(\theta_{mc} \leq 6.8^{\circ})$	3.0σ	2.4σ

- **This result indicates that a cosmic ray source may exist in the direction of PPSC.**

Li-Ma Significance Map with $E \geq 10^{19.6}$ eV

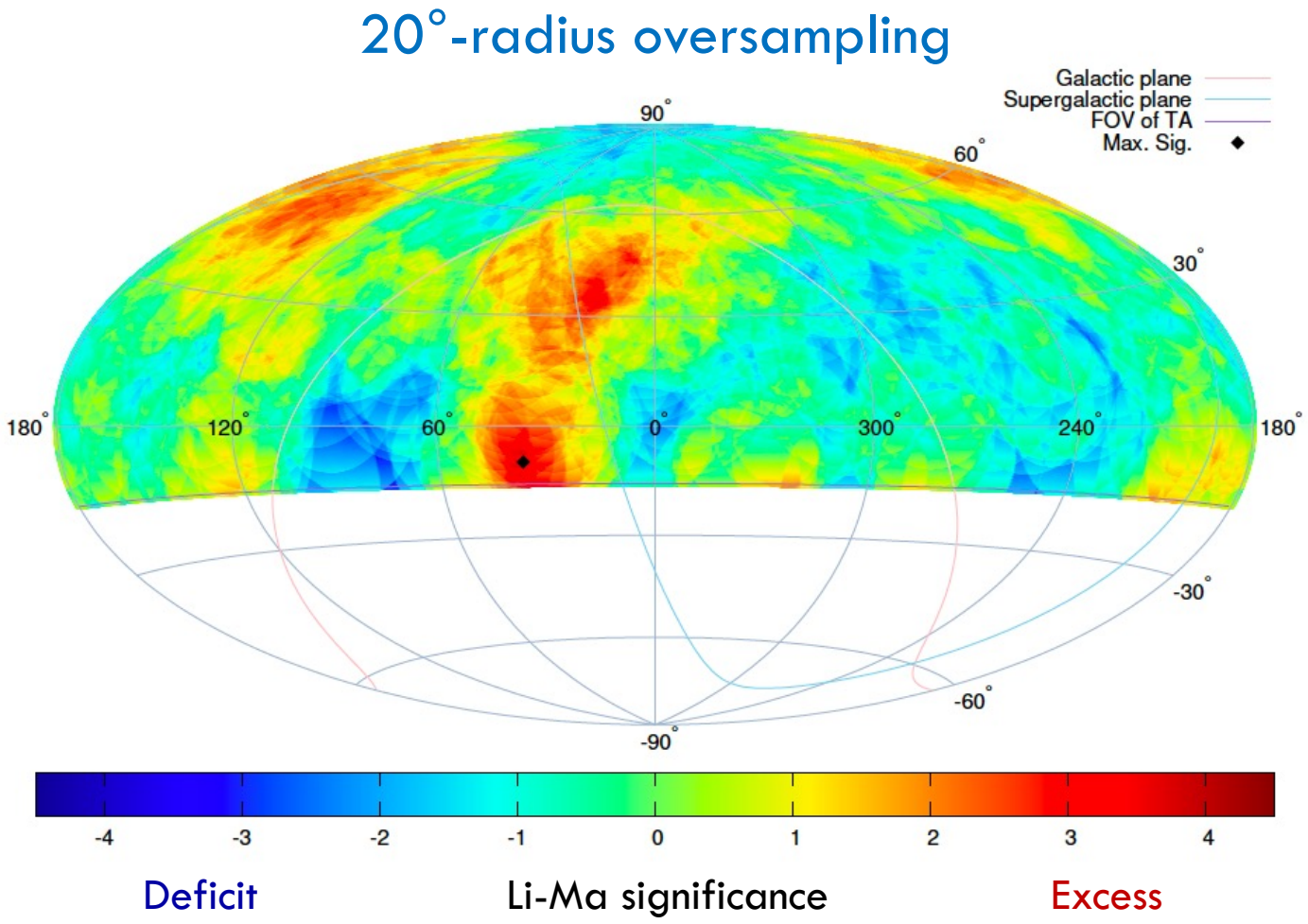

- 413 events (14-year TA SD data)

- Max local sig.: 3.9σ at (36.3°, -9.7°)
  - Obs.: 19 events
  - N_{bg}: 6.6 events
  - ~188% excess

- Local sig. at (19.7°, 34.6°): 3.5σ
  - Obs. : 43 events
  - N_{bg}: 23.2 events
  - ~85% excess

PPSC Excess Map with $E \geq 10^{19.6}$ eV + NGC 1068

NGC 1068
(40.67°, -0.013°)
14.4 Mpc

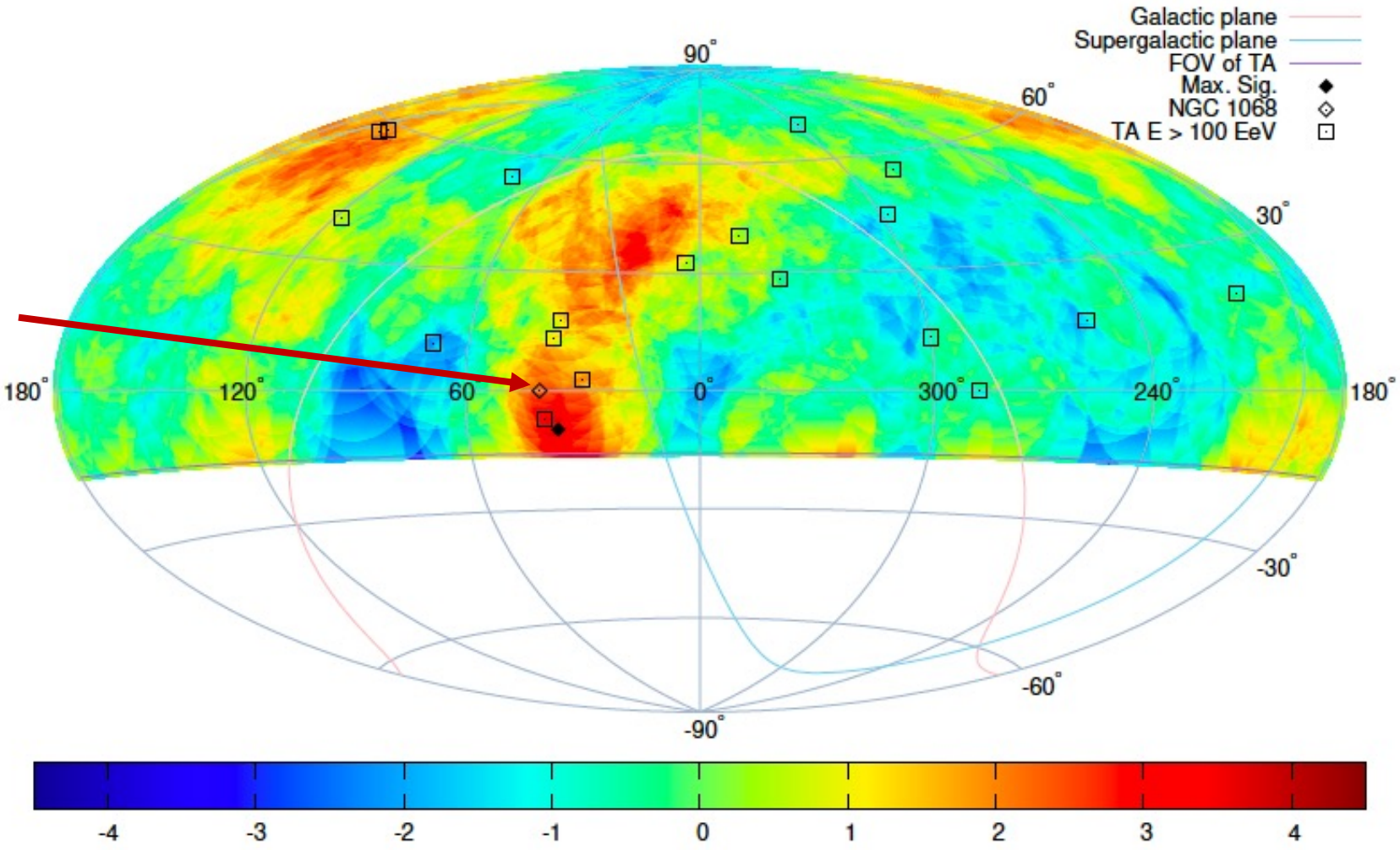

IceCube Collaboration, *Science* **378**, 538–543 (2022)

Evidence for neutrino emission from the nearby active galaxy NGC 1068

IceCube Collaboration*†

A supermassive black hole, obscured by cosmic dust, powers the nearby active galaxy NGC 1068. Neutrinos, which rarely interact with matter, could provide information on the galaxy's active core. We searched for neutrino emission from astrophysical objects using data recorded with the IceCube neutrino detector between 2011 and 2020. The positions of 110 known gamma-ray sources were individually searched for neutrino detections above atmospheric and cosmic backgrounds. We found that NGC 1068 has an excess of 79^{+22}_{-20} neutrinos at tera–electron volt energies, with a global significance of 4.2σ, which we interpret as associated with the active galaxy. The flux of high-energy neutrinos that we measured from NGC 1068 is more than an order of magnitude higher than the upper limit on emissions of tera–electron volt gamma rays from this source.

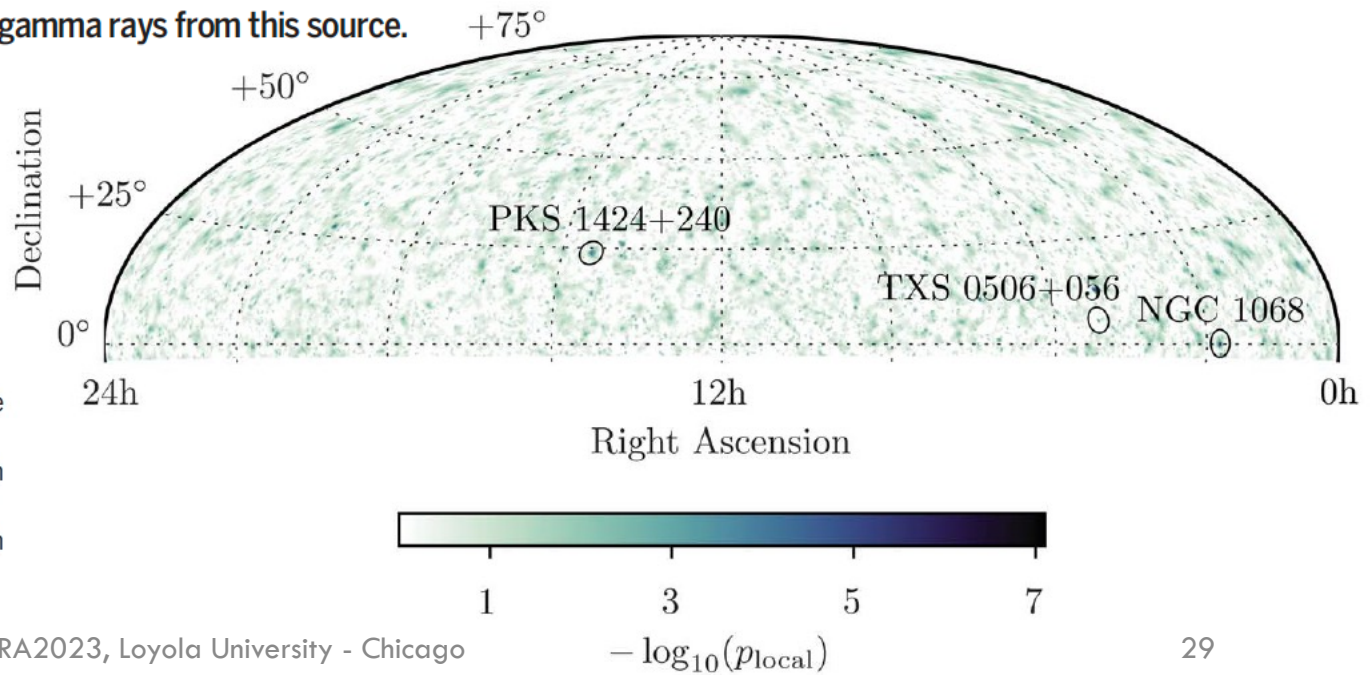

Fig. 1. Sky map of the scan for point sources in the Northern Hemisphere. The color scale indicates the logarithm of the local *P* value (P_{local}) obtained from our maximum likelihood analysis, evaluated (with the spectral index as a free parameter) at each location in the sky. The map is shown in equatorial coordinates on a Hammer-Aitoff projection. The black circles indicate the three most significant objects in the source list search, which are labeled. The circle around NGC 1068 contains the most significant location in the Northern Hemisphere, shown in higher resolution in Fig. 2A.

Li-Ma Significance Map with $E \geq 10^{19.6}$ eV

20°-radius oversampling

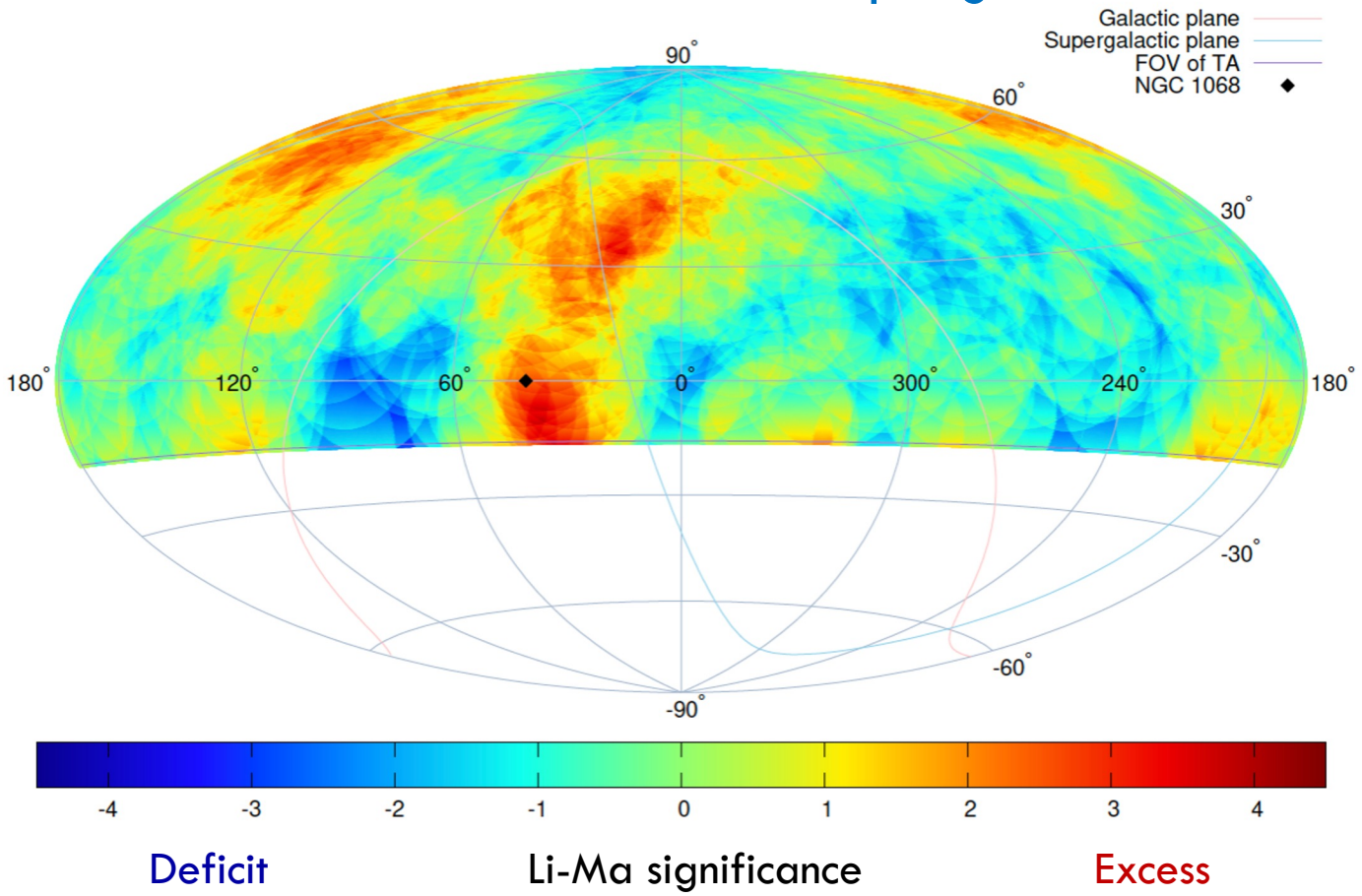

- 413 events (14-year TA SD data)

- Local significance at NGC 1068 coordinate (40.7°, 0°): **2.5σ**

Obs. : 21 events
N_{bg}: 11.4 events
} ~84% excess

Cosmic Rays from NGC 1068 assuming JF12 GMF Model

JF12 GMF

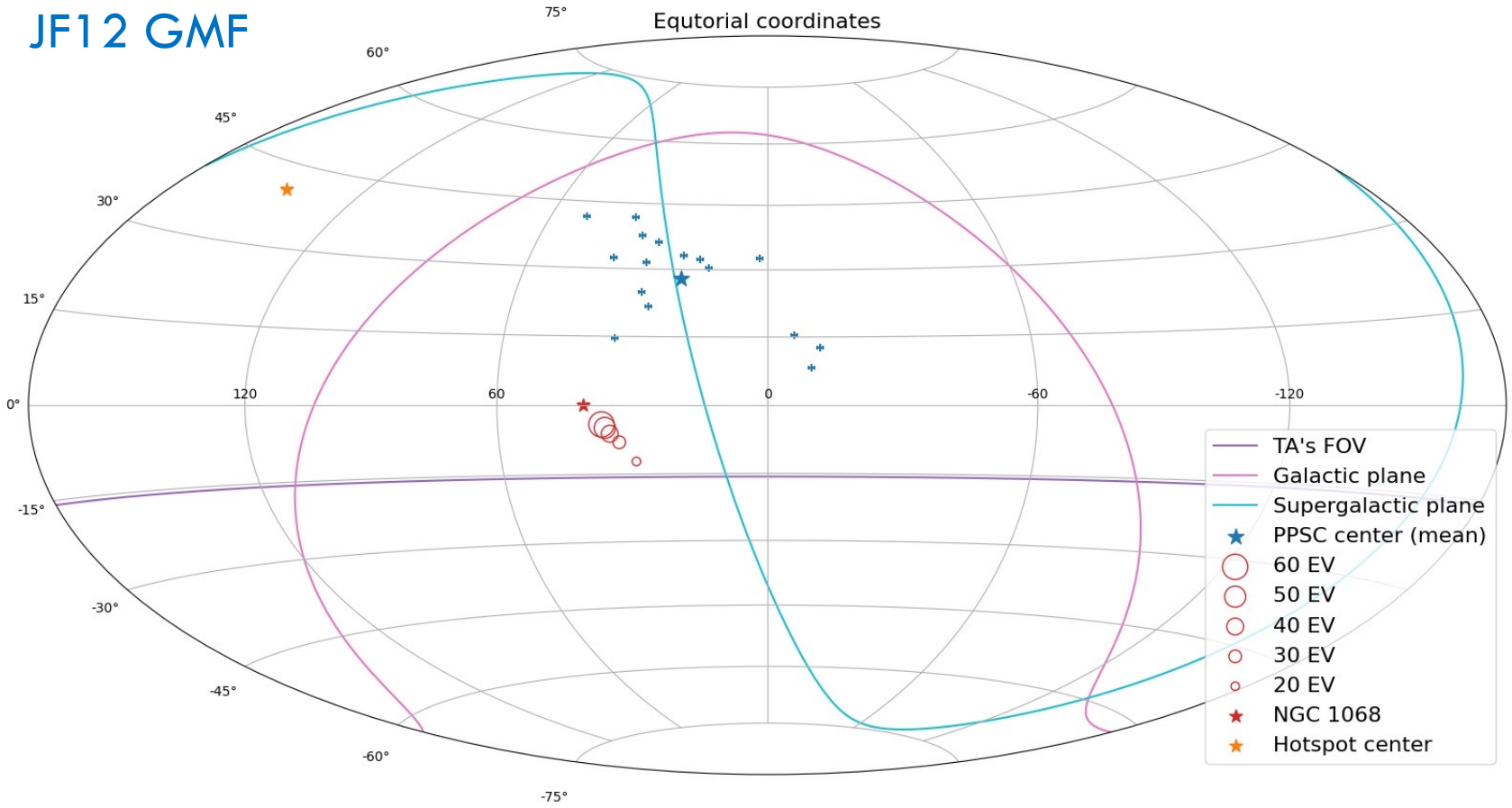

Cosmic Rays from NGC 1068 assuming JF12 GMF Model

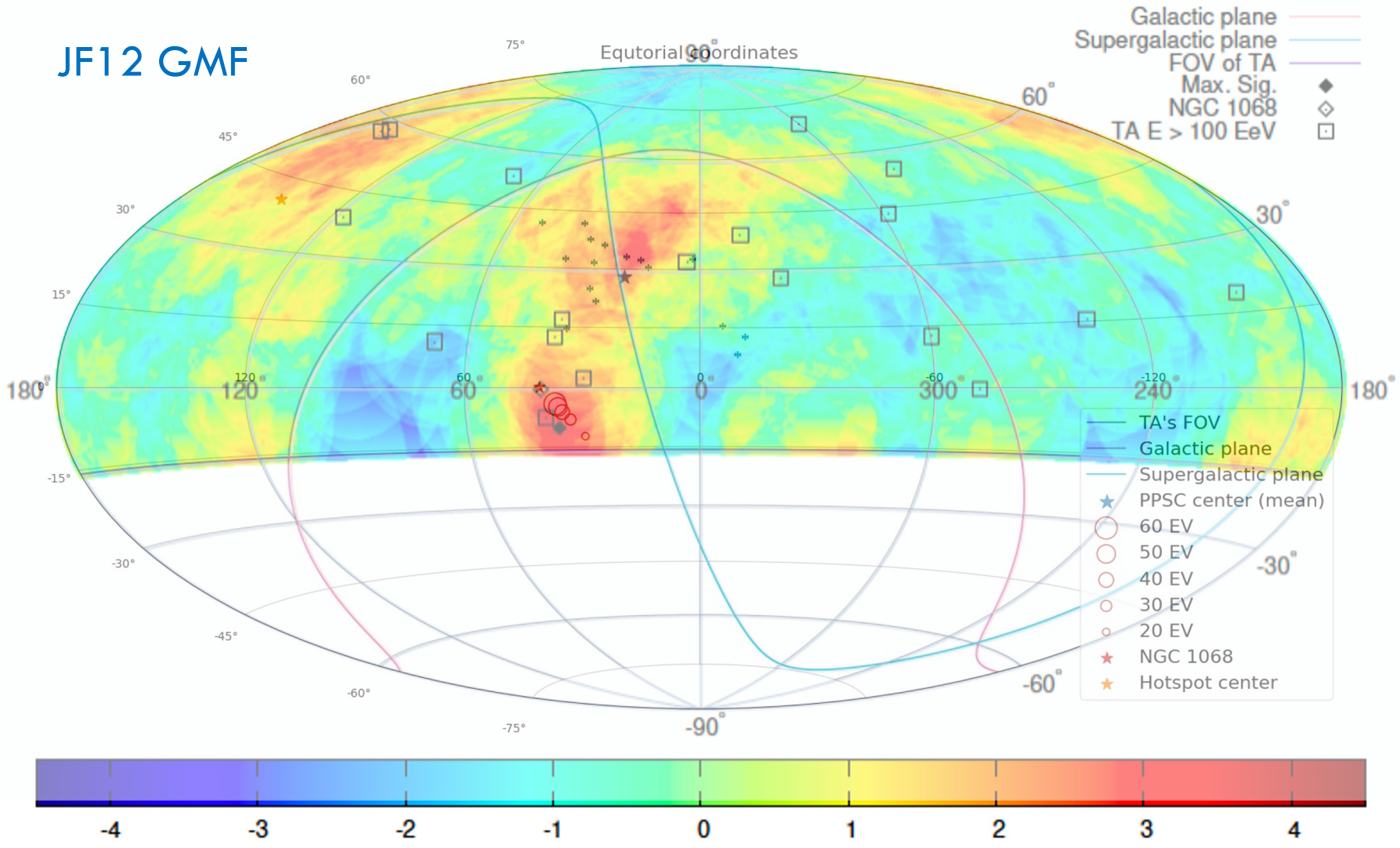

Cosmic Rays from NGC 1068 assuming PT11 GMF Model

PT11 GMF

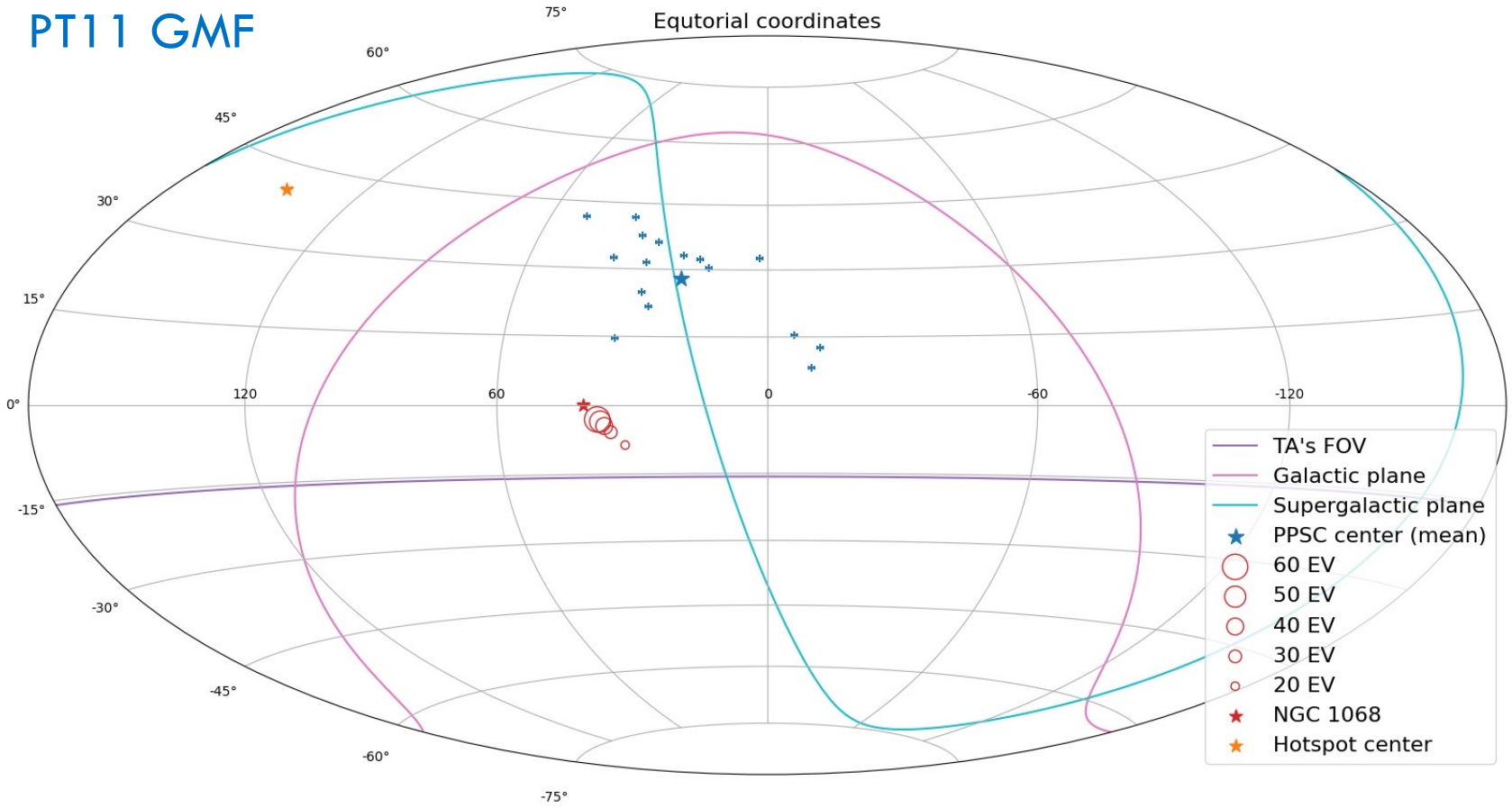

Cosmic Rays from NGC 1068 assuming PT11 GMF Model

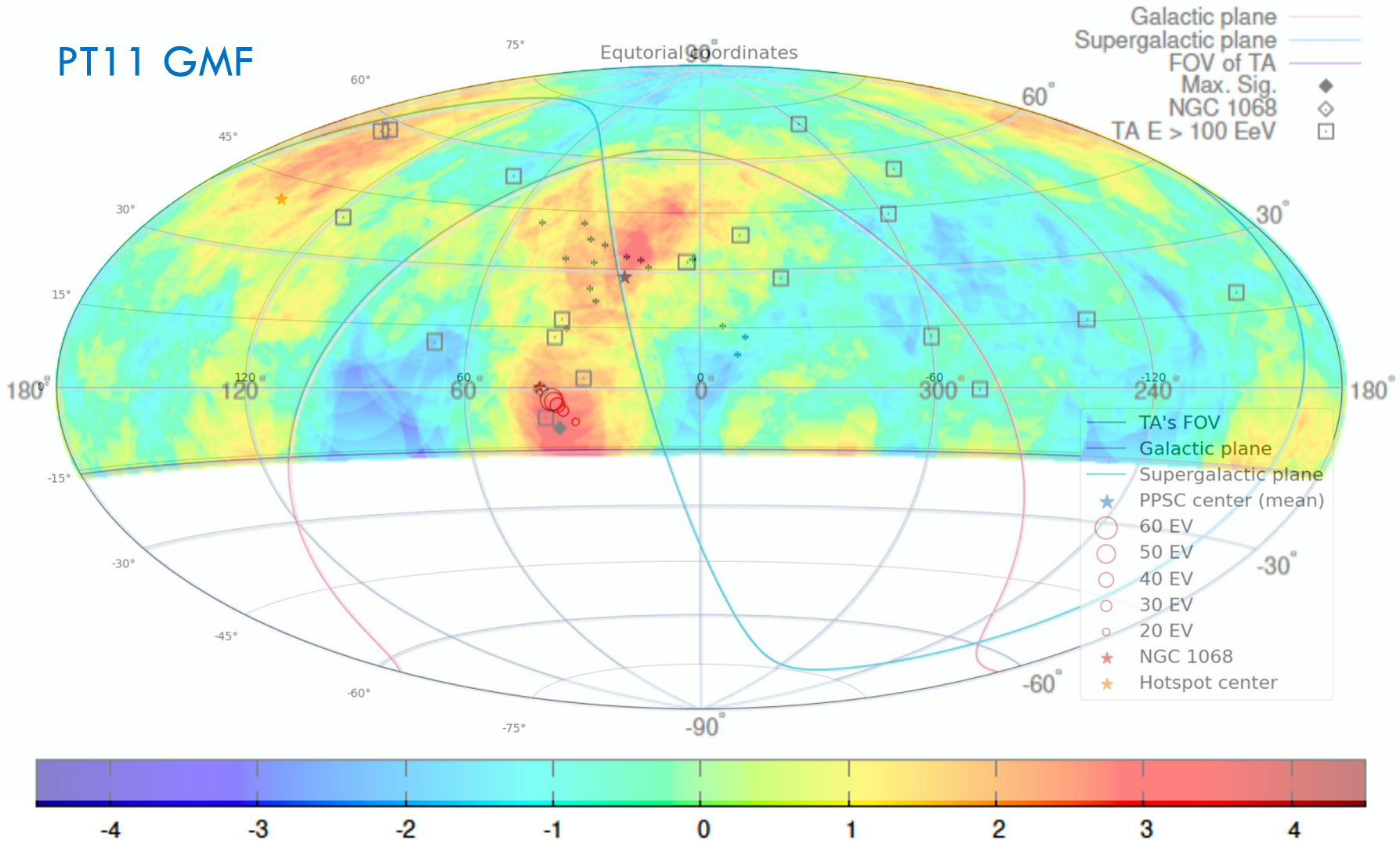

Summary

- We have persistent evidence for **the Hotspot** at the highest energies, $E \geq 5.7 \times 10^{19}$ eV, in the Ursa Major constellation. The global significance of such excess appearing by chance anywhere in TA's field of view is estimated to be **3.2σ.**
- A new excess in slightly lower energy events, $E \geq 10^{19.4}$ eV, in the direction of **the Perseus-Pisces supercluster** has been identified. The local significance of excess is estimated to be **3.8σ**. The chance probability of having an excess as close to the PPSC as the data is estimated to be **3.1σ.**
- It indicates that **a cosmic ray source may exist in the direction of PPSC**, which is the closest supercluster other than the Local supercluster where we reside and is next to the Local Void where the magnetic field strength is presumed to be weaker than other structures in the cosmic web. It is important to study astronomical objects in the supercluster further and to increase the statistical power of northern hemisphere cosmic ray studies.
- The four-fold extension of the Telescope Array experiment, **the TA×4 project**, will accelerate data taking.

TA×4 project: Upgraded!!!

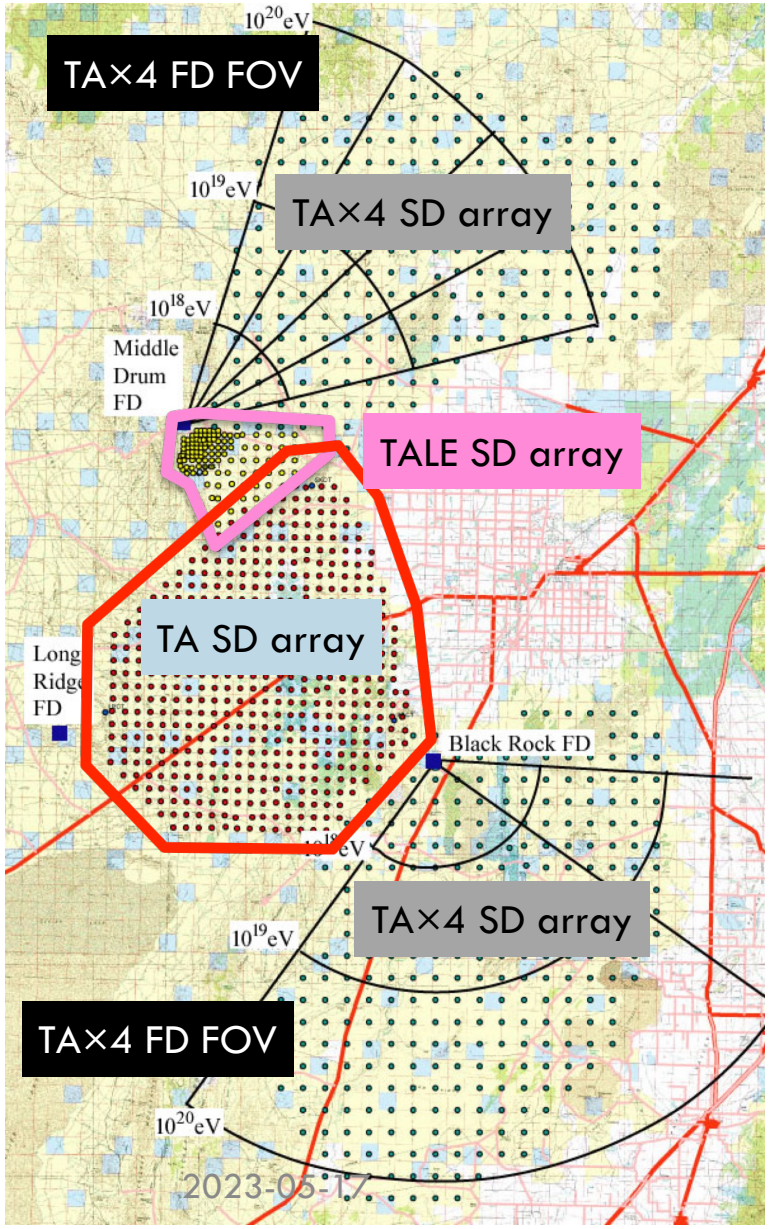

- Motivation
  To study more about the highest energies and examine the implications obtained by TA
- Four times TA SD (**~3000 km^2**)
  500 new SDs with 2.08 km spacing
- Two FD stations
  North/South stations were installed now.
- Status
  - ~250 TAx4 SDs were deployed in Mar. 2019.
  - Two TAx4 FD stations were constructed.
  - Data acquisition has been started.
- Prospects
  Gives us a crucial clue to identify UHECR sources with high statistics

Backup

Perseus-Pisces Supercluster

- It is found that the place where the new excess of events appears is in the region of the Perseus-Pisces supercluster (PPSC), which is one of the notable structures in TA's field of view.
- The PPSC is the closest supercluster other than the local supercluster we reside in. Also, it is known that it has a gigantic filamentary structure, stretching for over 300 Mpc/h (Batuski & Burns 1985)
- According to Haynes and Giovanelli (Haynes & Giovanelli 1986), the major portion of the foreground between the earth and the PPSC, and also of that beyond the PPSC, are nearly empty.
- Courtois et al. provide density contour maps after making corrections for catalog incompleteness (Courtois et al. 2013). Fig. 8 in this paper shows that the PPSC is clearly seen as an elongated structure of galaxies. In the direction of the new excess of events, no prominent structures between the earth and the PPSC, or beyond the PPSC, are seen.
- If the new excess of events in arrival direction distribution is real, the PPSC could be responsible for it.

Perseus-Pisces Supercluster

- Perseus-Pisces supercluster consists of three main clusters and some groups of galaxies.

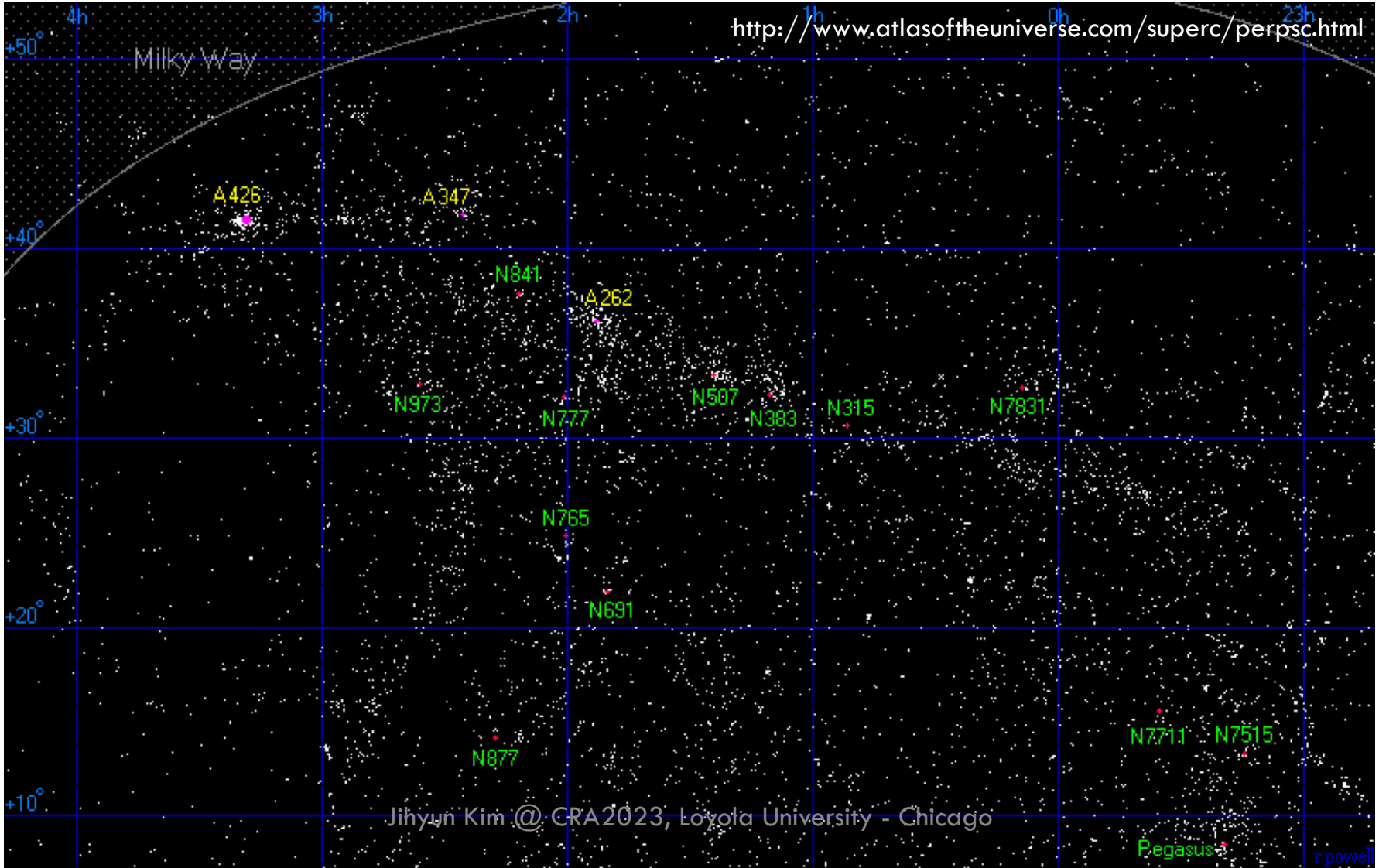

The PPSC is a unique and significant structure in TA's field of view because it is the **closest** supercluster other than the Local supercluster where we reside, and its location is **next to the Local Void** where the magnetic field strength is presumed to be weaker than other structures in the cosmic web.

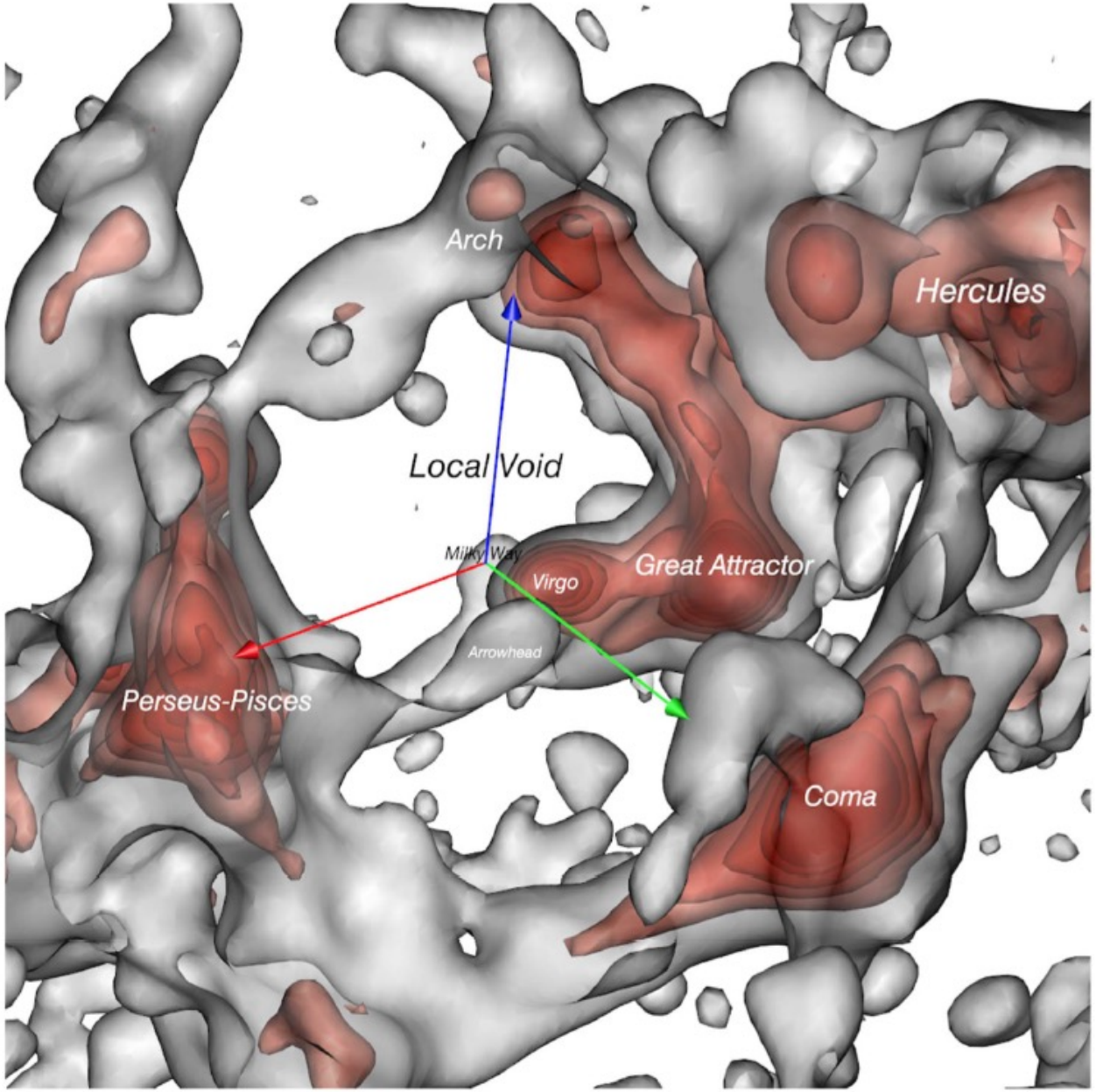

Figure 1. Overview of the structure surrounding the Local Void. Isosurfaces of density are inferred from the velocity field constructed from the Wiener Filter treatment of Cosmicflows distances, with the densest peaks in red and less dense filaments in gray. The Milky Way is at the origin of the colored arrows, 5000 km s^{-1} in length, oriented in the frame of supergalactic coordinates (red toward +SGX, green toward +SGY, blue toward +SGZ). The Local Void fills the empty region above the Milky Way in this plot. This view inward from a location at positive values of SGX, SGY, and SGZ will be referred to as the reference orientation.

Tully et al. (2019)

"The northern puck is dominated by the LSC at the center, the Great Wall (now straight in this cylindrical projection) at 10–14.5 hr, and Pisces-Perseus at 0–5 hr."

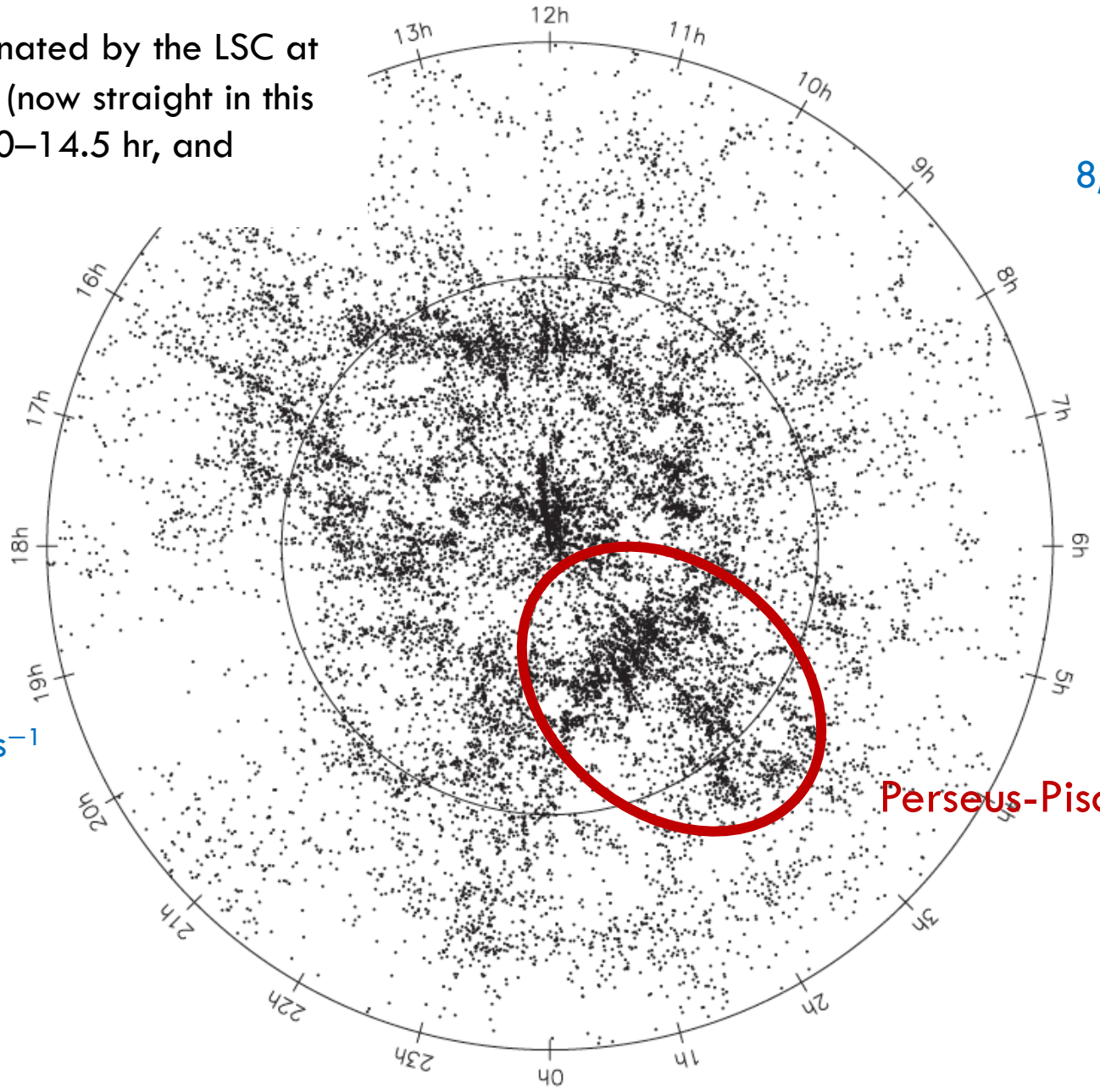

8,000 km s^{-1}

Hockey Puck
Northern hemisphere

15,000 km s^{-1}
(~200 Mpc)

Perseus-Pisces supercluster

Figure 7. Hockey Puck plot—a full cylinder section—of 2MRS in the north celestial cap. The view is looking downward from the NCP, the thickness of the "puck" is 8000 km s^{-1}, and its radius is 15,000 km s^{-1}.

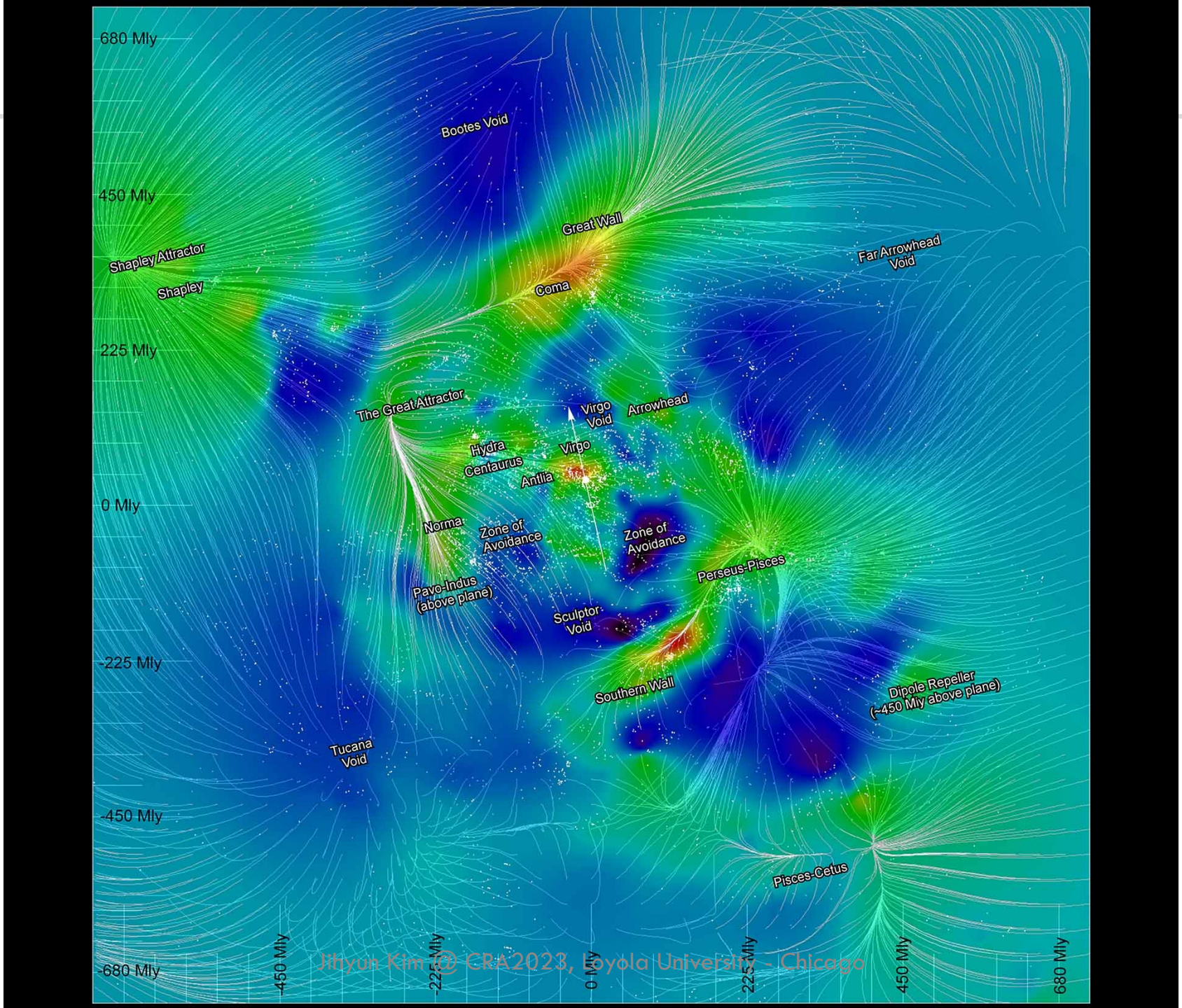
680 Mly
450 Mly
225 Mly
0 Mly
-225 Mly
-450 Mly
-680 Mly
Bootes Void
Great Wall
Shapley Attractor
Shapley
Coma
Far Arrowhead Void
The Great Attractor
Virgo Void
Arrowhead
Hydra
Virgo
Centaurus
Antlia
Norma
Zone of Avoidance
Zone of Avoidance
Perseus-Pisces
Pavo-Indus (above plane)
Sculptor Void
Southern Wall
Dipole Repeller (~450 Mly above plane)
Tucana Void
Pisces-Cetus
-450 Mly
-225 Mly
0 Mly
225 Mly
450 Mly
680 Mly

~208 Mpc

Mapping of rich superclusters within ~460 Mpc

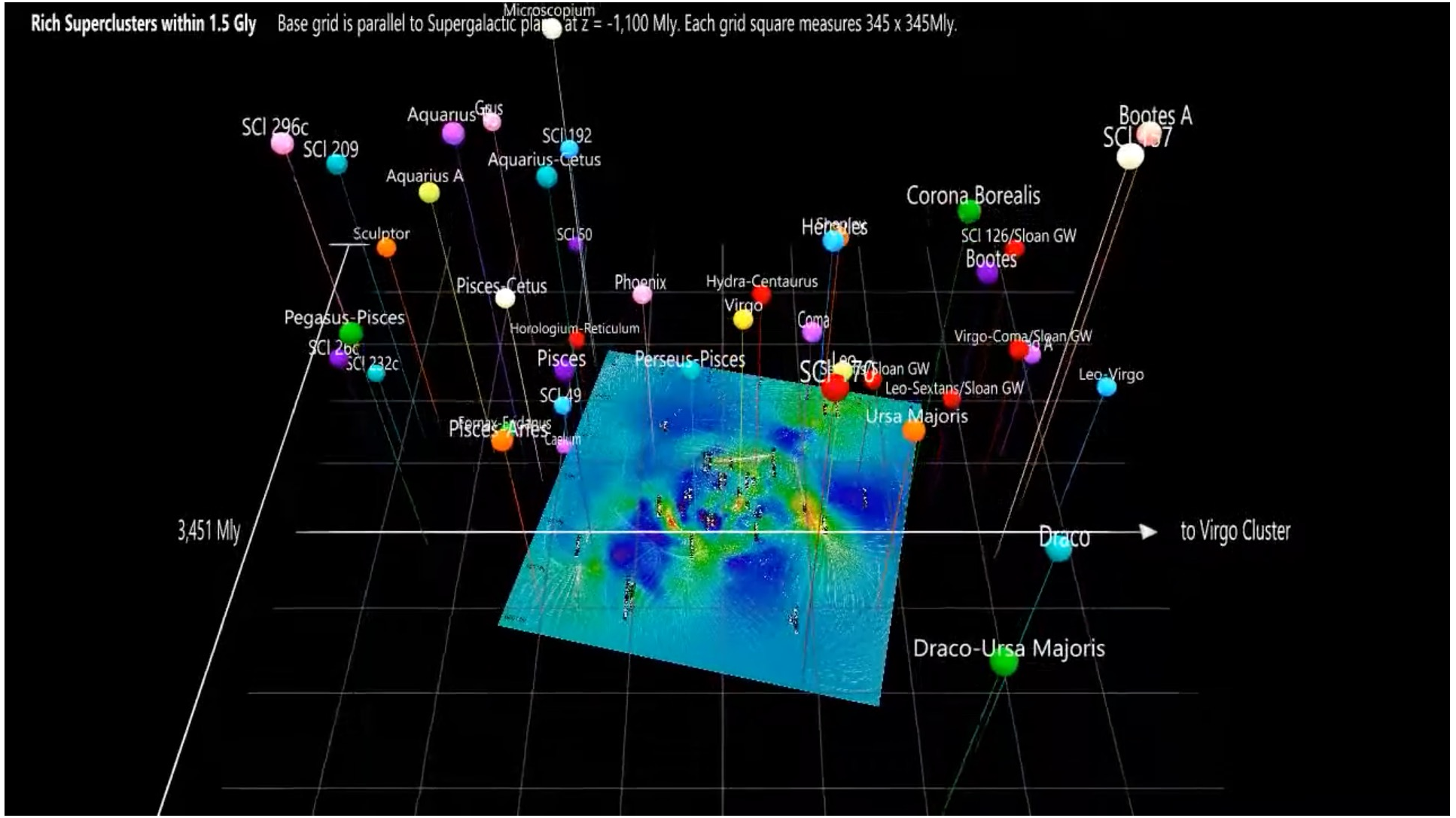

http://www.galaxies3d.org/bey-rich-superclusters.htm

Six filaments of galaxies connected to the Virgo cluster

black dots: TA 5-year data TA (2014)
color dots: filaments of galaxies S. Kim+ (2016)
gray dots: local galaxies Makarov+ (2014)

JK+(2019)

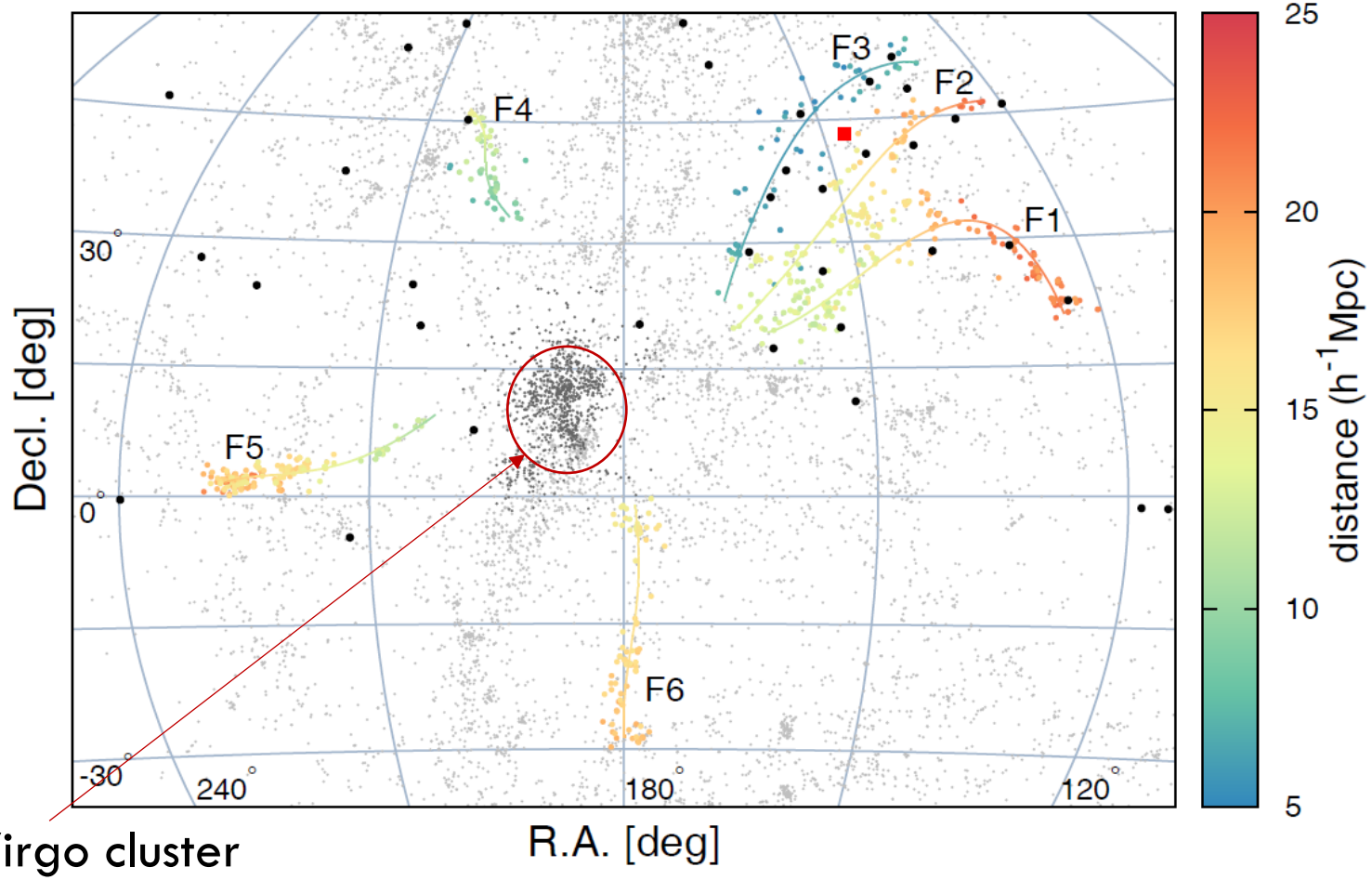

The Virgo cluster

Close correlation between TA events and filaments

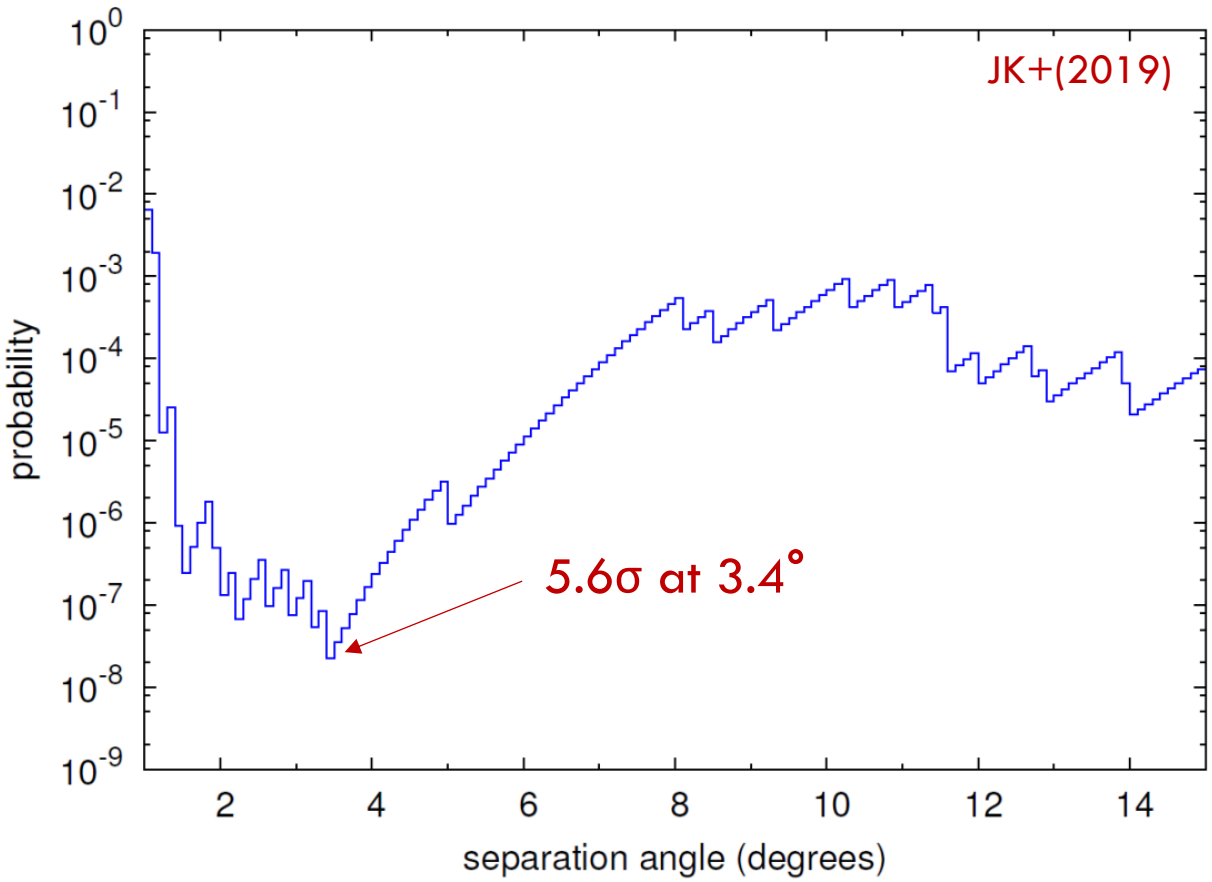

- 72 events with E > 5.7×10^{19} eV
  (5-year TA SD data)
- Maximum local significance: 5.6σ
  Observed: 19 events
  Expected from iso.: 4.2 events } ~350% excess
- Post-trial probability: $P(\mathrm{p_{pre}} > 5.6\sigma) = 5.1\sigma$

- **A close correlation** with astronomical objects with such high significance
- The estimated mass composition of UHECRs and the strength of galactic magnetic fields are consistent with observations.

A plausible model for the origin of TA hotspot

JK+(2019)

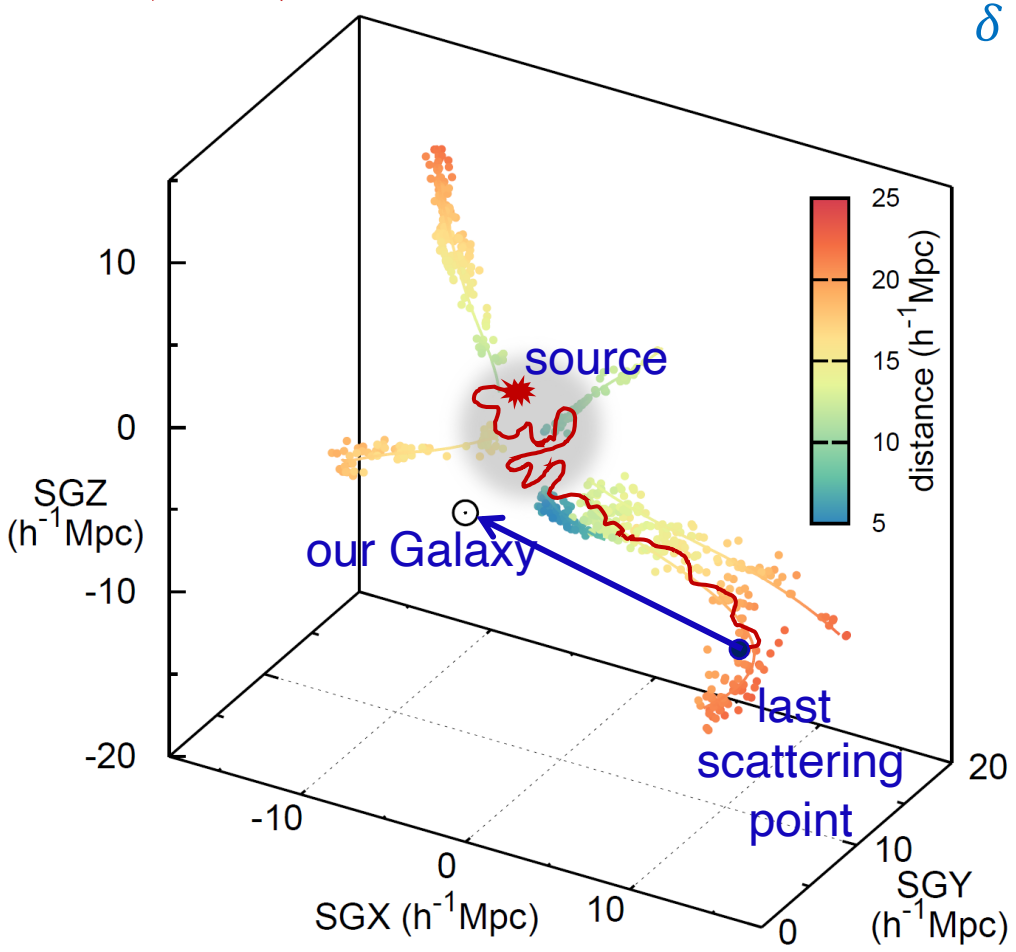

$$\delta \sim f \times \frac{\pi}{2}\left(\frac{5\times10^{19}\ \mathrm{eV}}{E/Z}\right)\left(\frac{L}{25\ \mathrm{Mpc}}\right)^{1/2}\left(\frac{l_c}{1\ \mathrm{Mpc}}\right)^{1/2}\left(\frac{B_{\mathrm{random}}}{20\ \mathrm{nG}}\right)$$

- UHECRs are postulated to be produced at a source (sources) inside the Virgo cluster. They roam around for a while because of cluster magnetic fields. Then, some of them escape through connected filaments.
- This picture requires
  - B >~1 μG in clusters
  - B > ~20 nG in filaments
  - (Size of cluster/filament ~ a few Mpc)